

# 2023 at CRIS

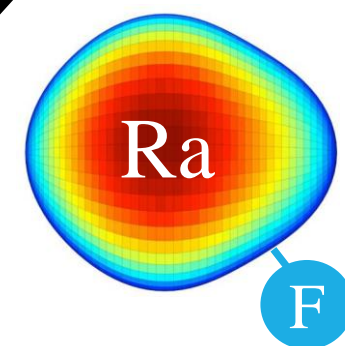
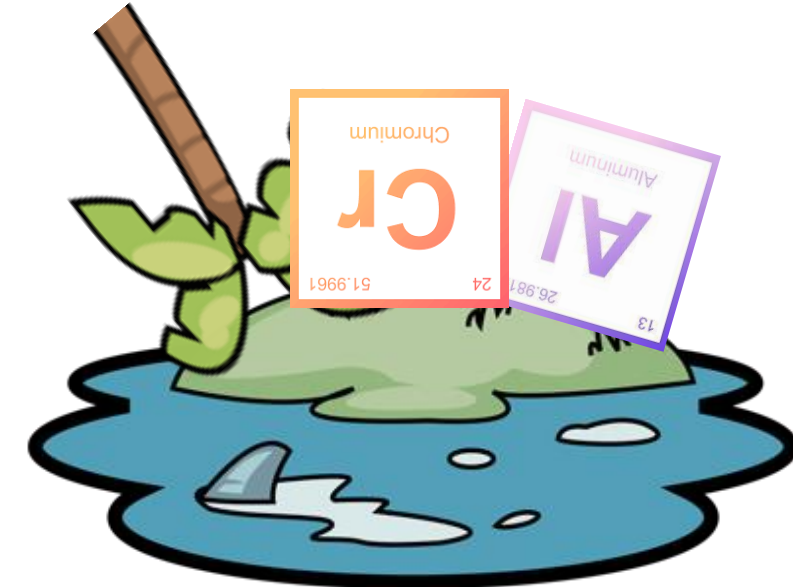
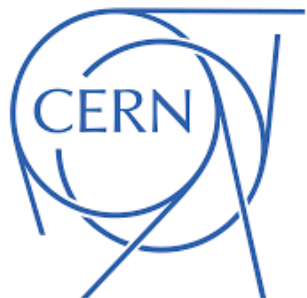
Louis Lalanne

CERN / ISOLDE

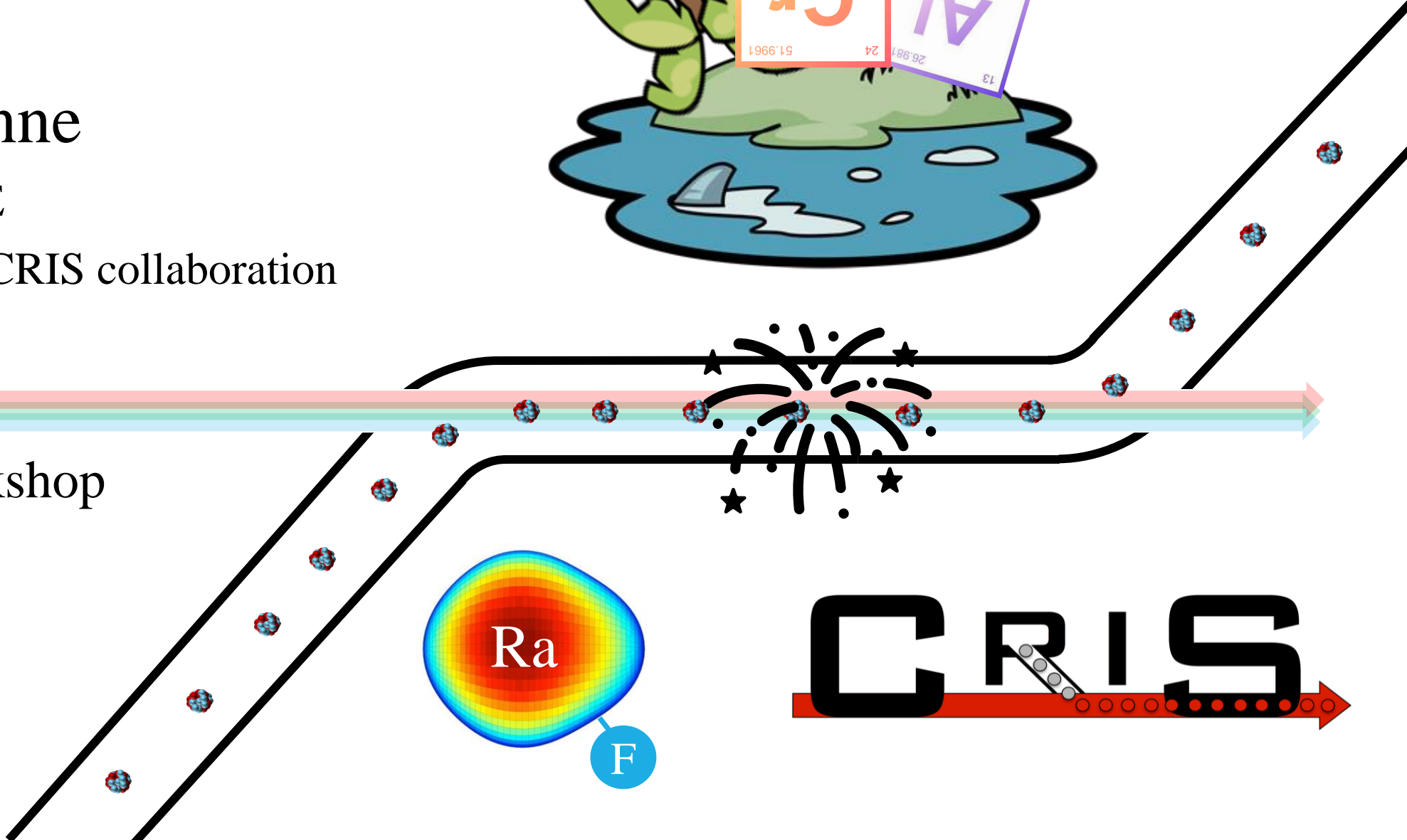
on behalf of the CRIS collaboration

ISOLDE Workshop

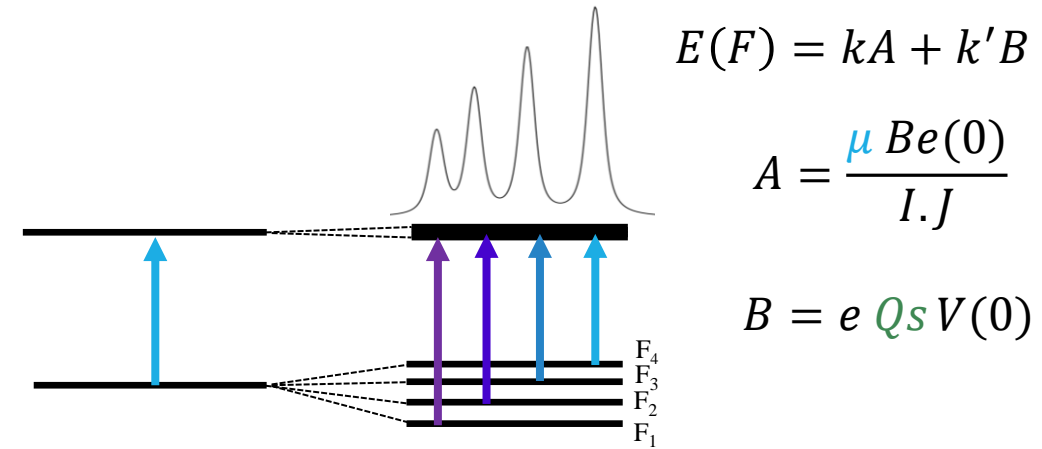
30/11/2023



**CRIS**



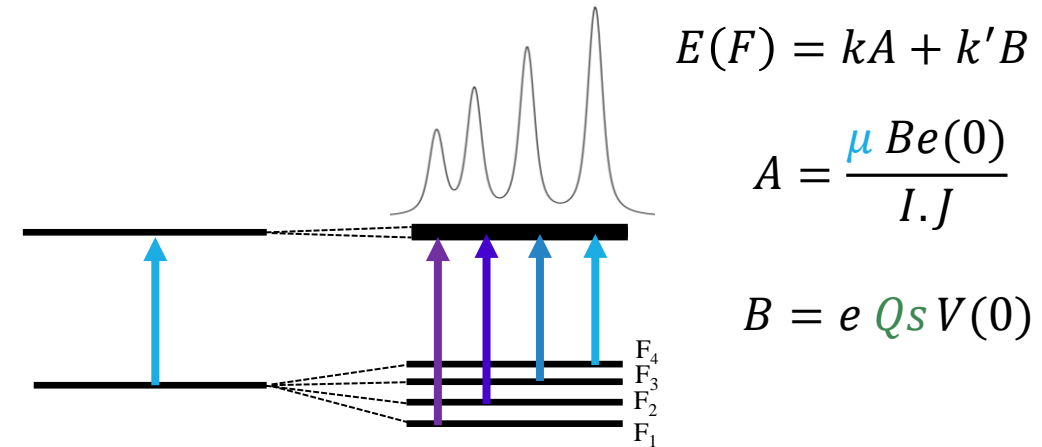
CRIS : Collinear Resonance Ionization Spectroscopy



Isotope shift : shift of HFS between two isotopes A and A'

$$\delta\nu_i^{A,A'} = \frac{A - A'}{AA'} M_i + F_i \delta\langle r^2 \rangle^{AA'}$$

## CRIS : Collinear Resonance Ionization Spectroscopy

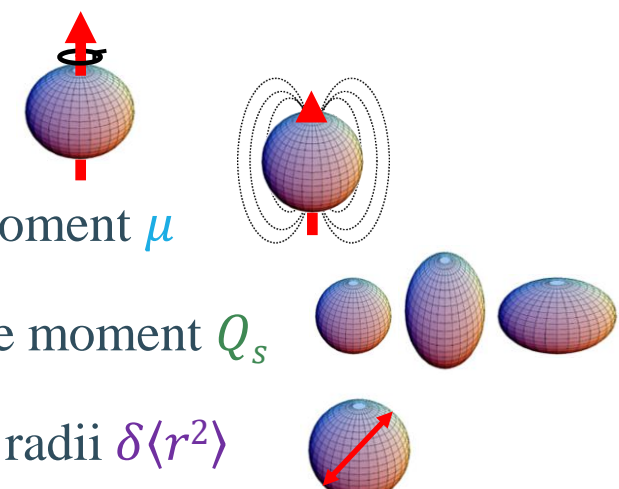


Isotope shift : shift of HFS between two isotopes A and A'

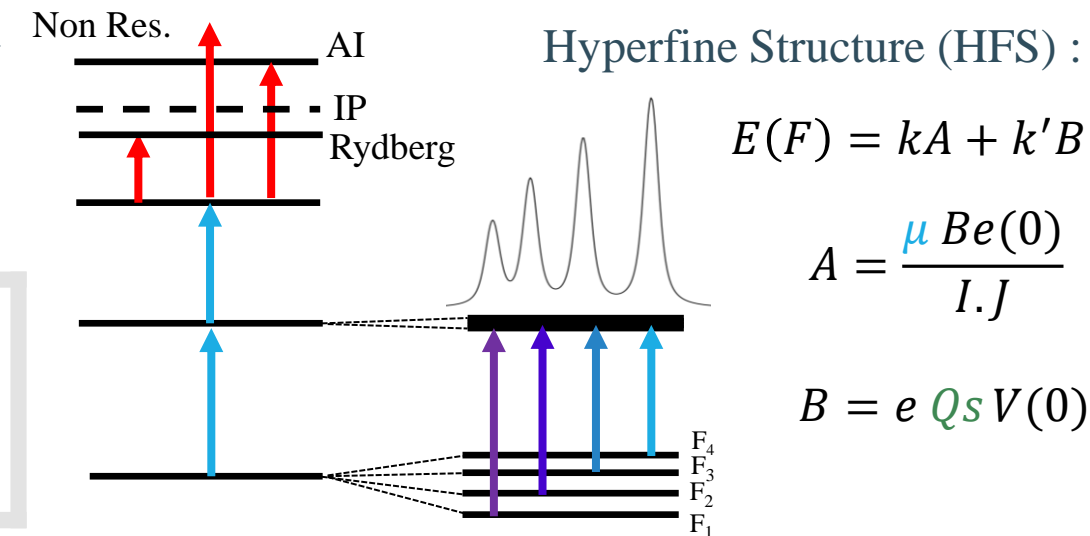
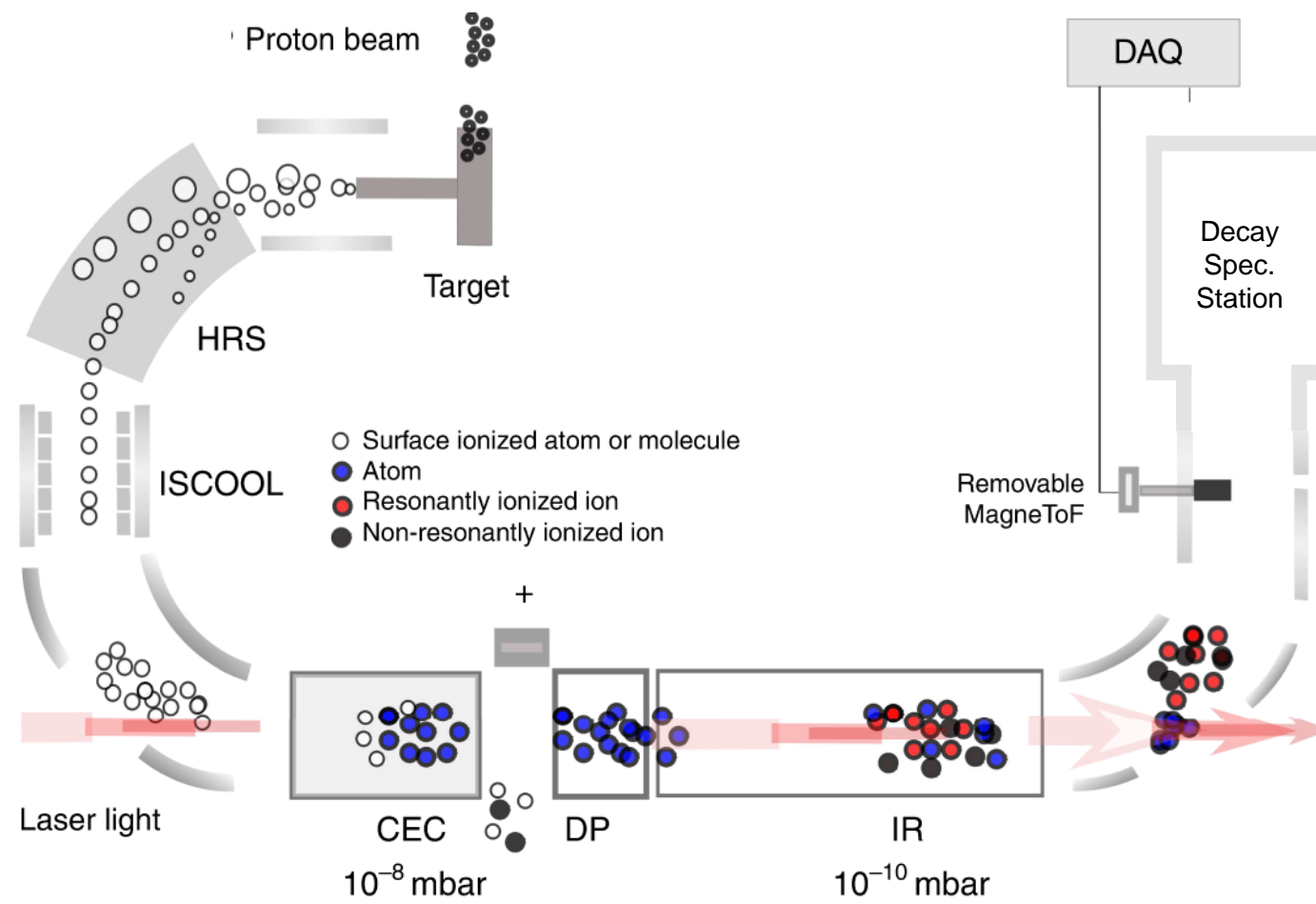
$$\delta\nu_i^{A,A'} = \frac{A - A'}{AA'} M_i + F_i \delta\langle r^2 \rangle^{AA'}$$

Measuring the HFS :

- Nuclear Spin I
- Magnetic dipole moment  $\mu$
- Electric quadrupole moment  $Q_s$
- Changes of charge radii  $\delta\langle r^2 \rangle$



## CRIS : Collinear Resonance Ionization Spectroscopy

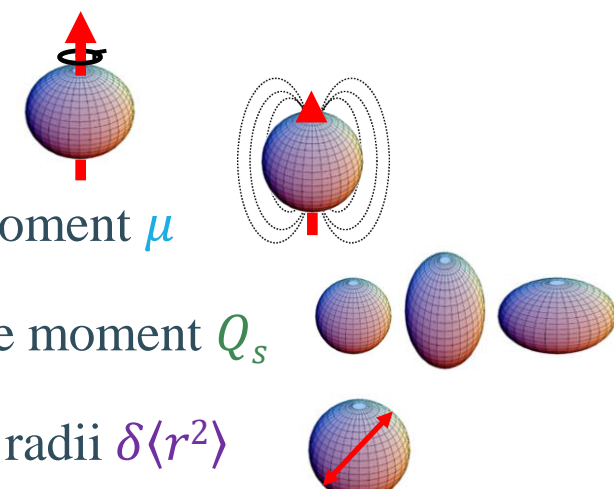


Isotope shift : shift of HFS between two isotopes A and A'

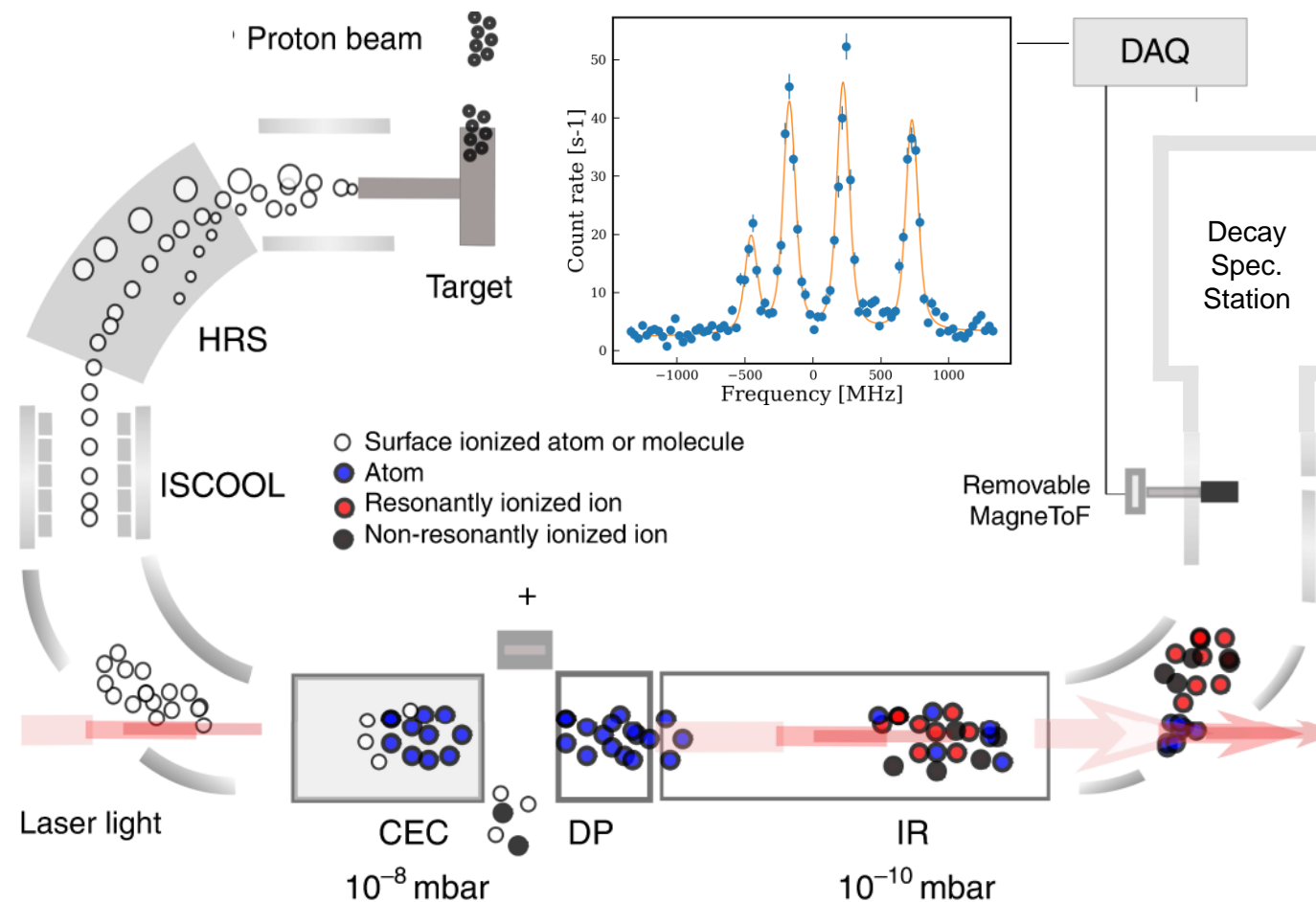
$$\delta\nu_i^{A,A'} = \frac{A - A'}{AA'} M_i + F_i \delta\langle r^2 \rangle^{AA'}$$

Measuring the HFS :

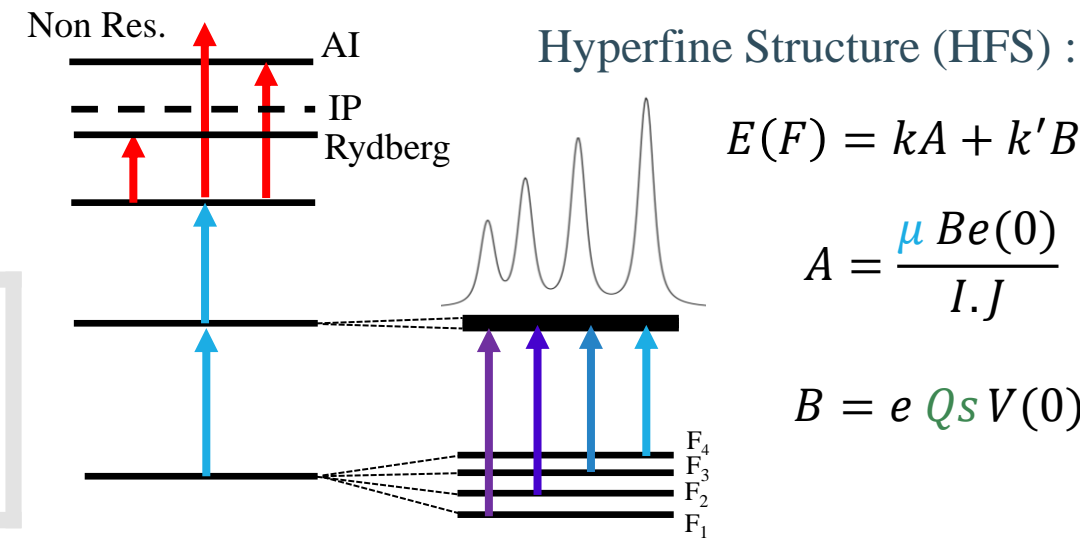
- Nuclear Spin I
- Magnetic dipole moment  $\mu$
- Electric quadrupole moment  $Q_s$
- Changes of charge radii  $\delta\langle r^2 \rangle$



## CRIS : Collinear Resonance Ionization Spectroscopy



- ✓ High sensitivity : > few 10 ions/s
- ✓ High resolution : > 20 MHz
- ✓ High versatility



Isotope shift : shift of HFS between two isotopes A and A'

$$\delta\nu_i^{A,A'} = \frac{A - A'}{AA'} M_i + F_i \delta\langle r^2 \rangle^{AA'}$$

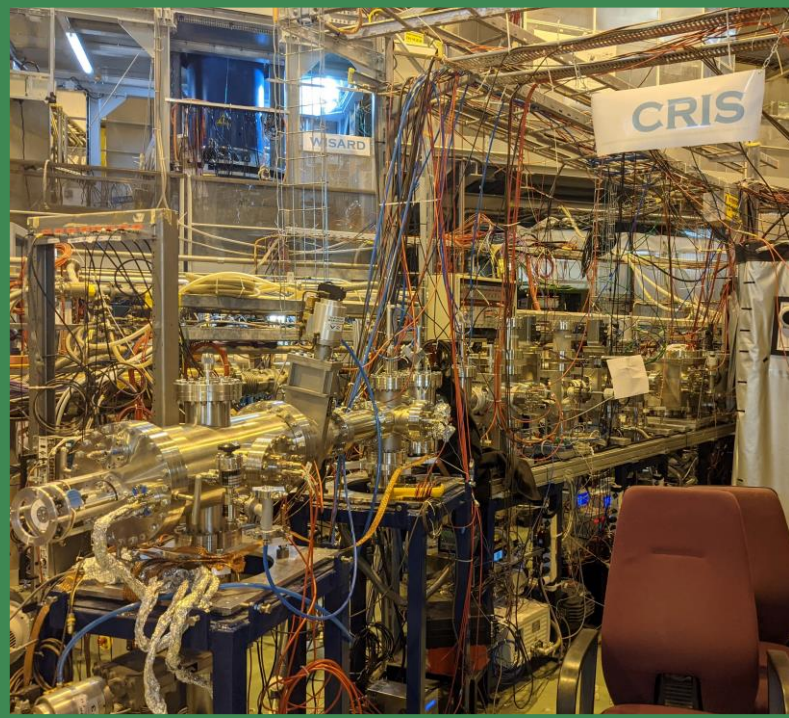
Measuring the HFS :

- Nuclear Spin  $I$
  - Magnetic dipole moment  $\mu$
  - Electric quadrupole moment  $Q_s$
  - Changes of charge radii  $\delta\langle r^2 \rangle$
-

# 2023 CRIS upgrade: New End of the Beam Line

6

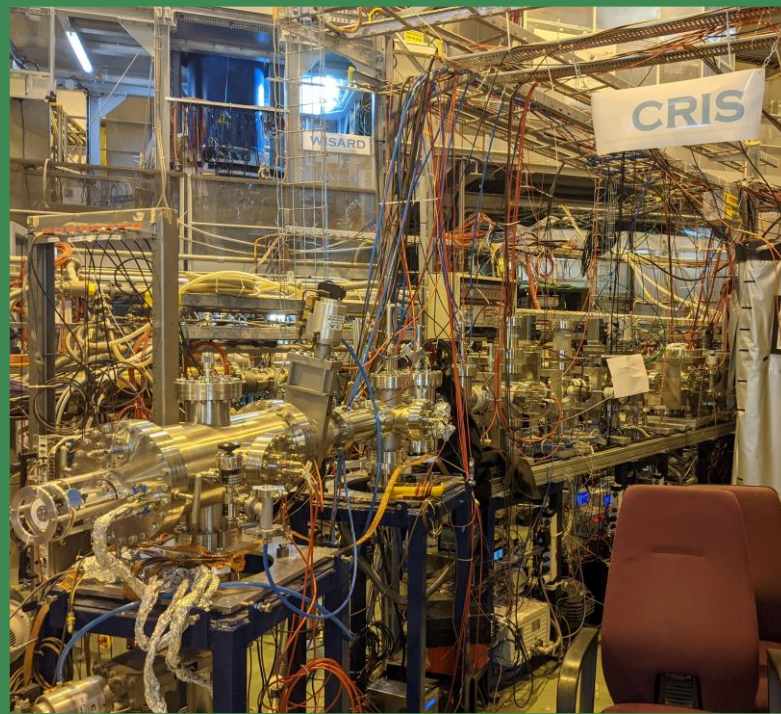
Decembre 2022



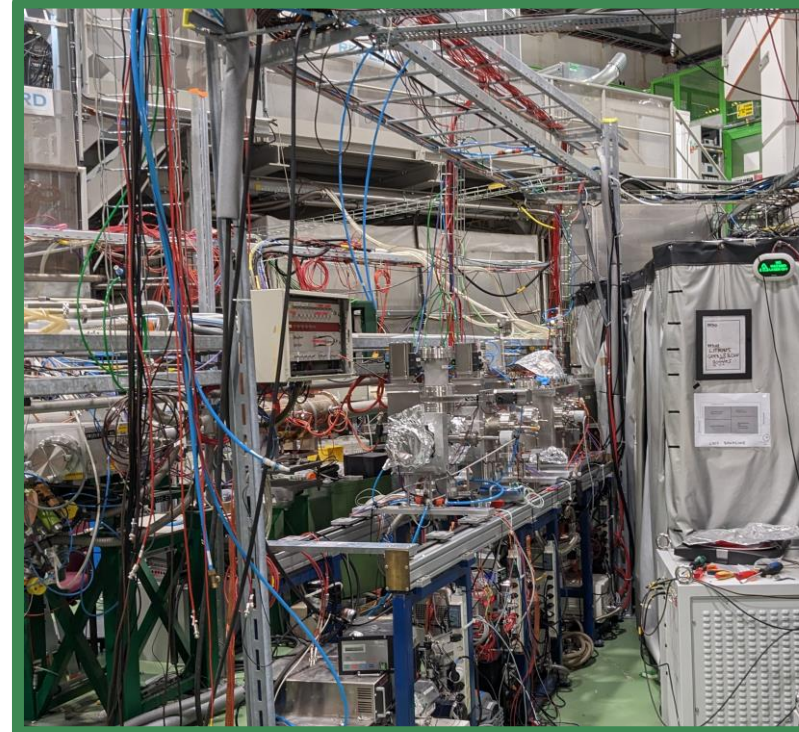
# 2023 CRIS upgrade: New End of the Beam Line

7

Decembre 2022



January 2023



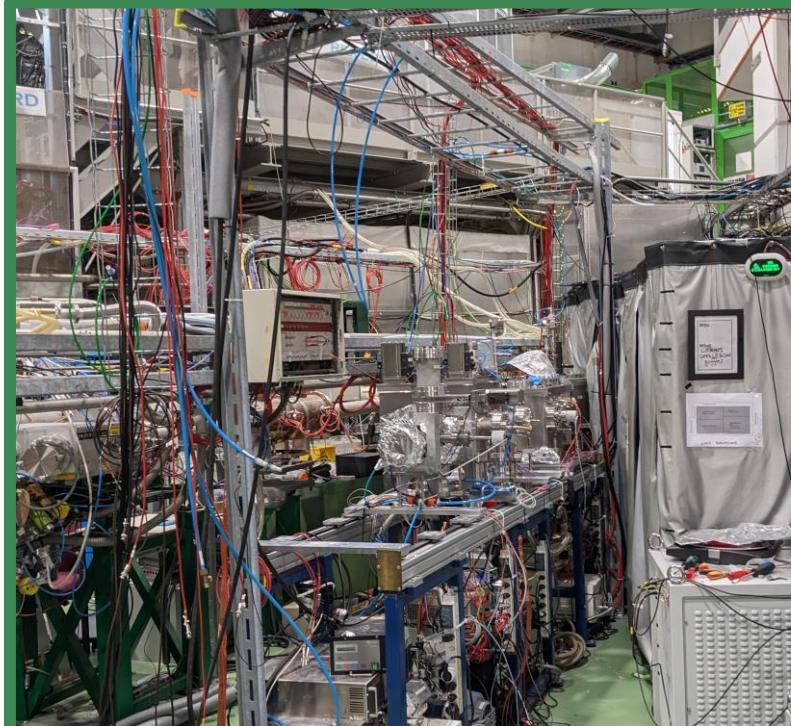
# 2023 CRIS upgrade: New End of the Beam Line

8

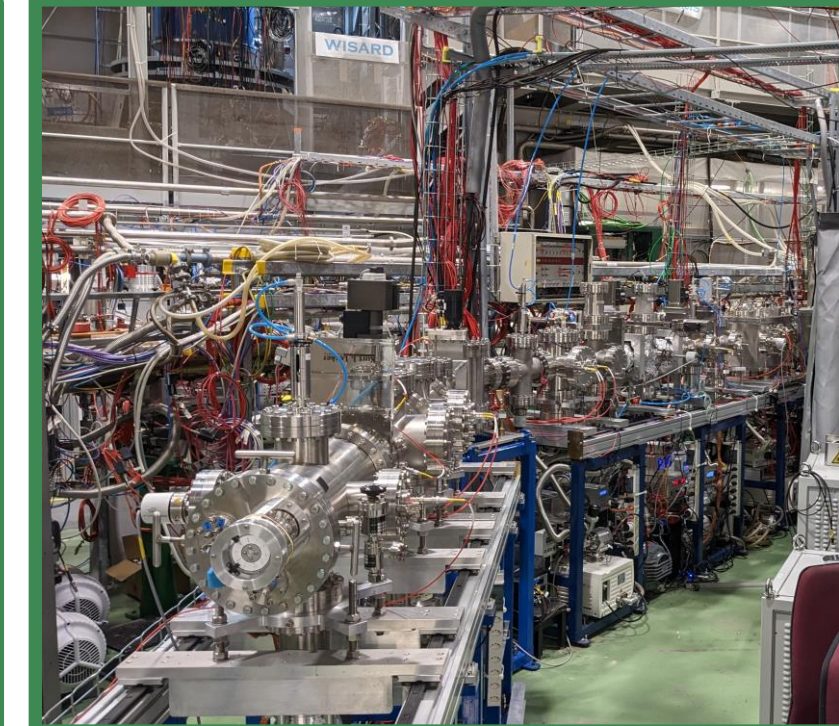
Decembre 2022



January 2023



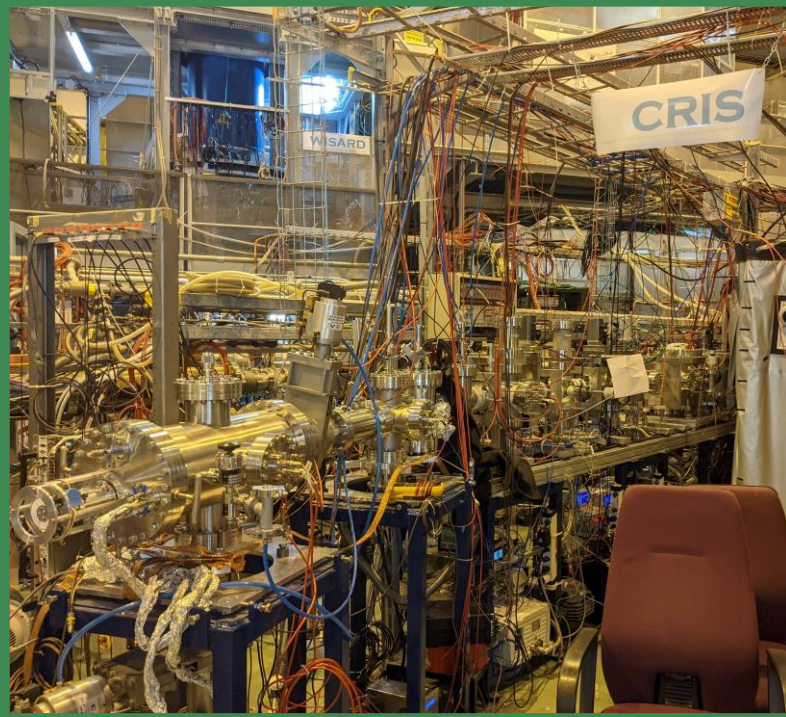
March 2023



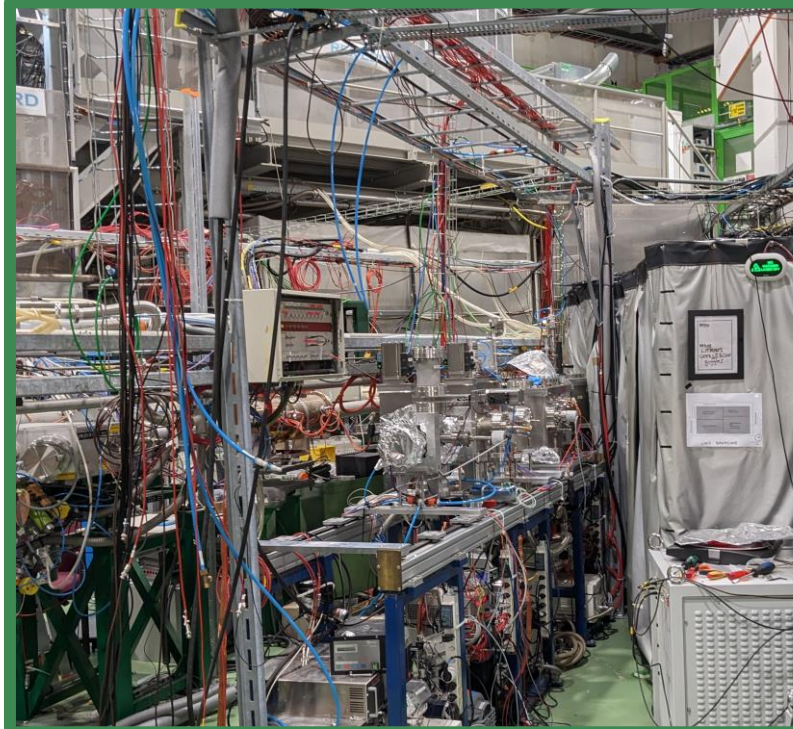
# 2023 CRIS upgrade: New End of the Beam Line

9

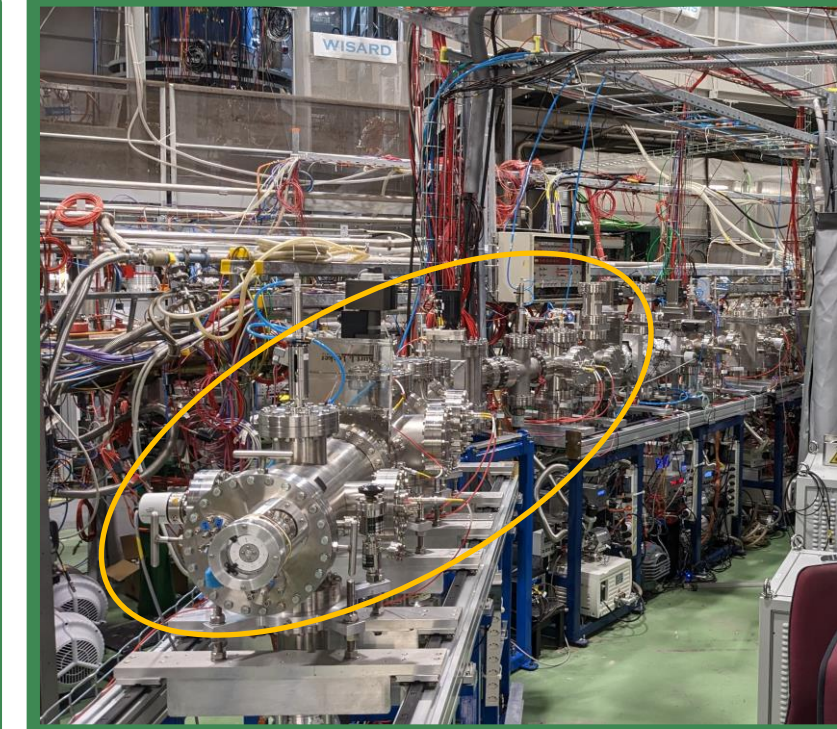
December 2022



January 2023



March 2023



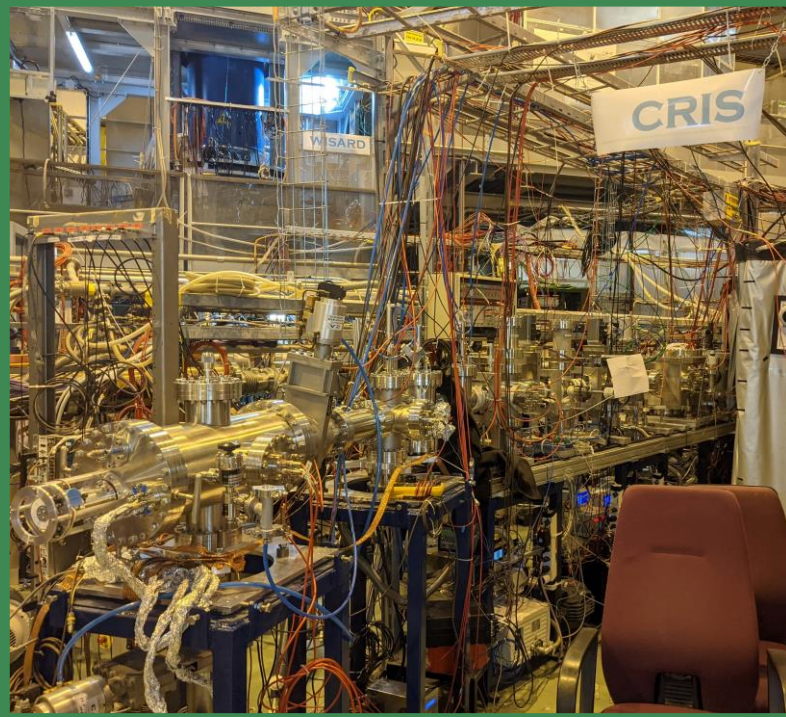
## New end of the beam line:

- New field ionization unit
- New bender
- New beam optics

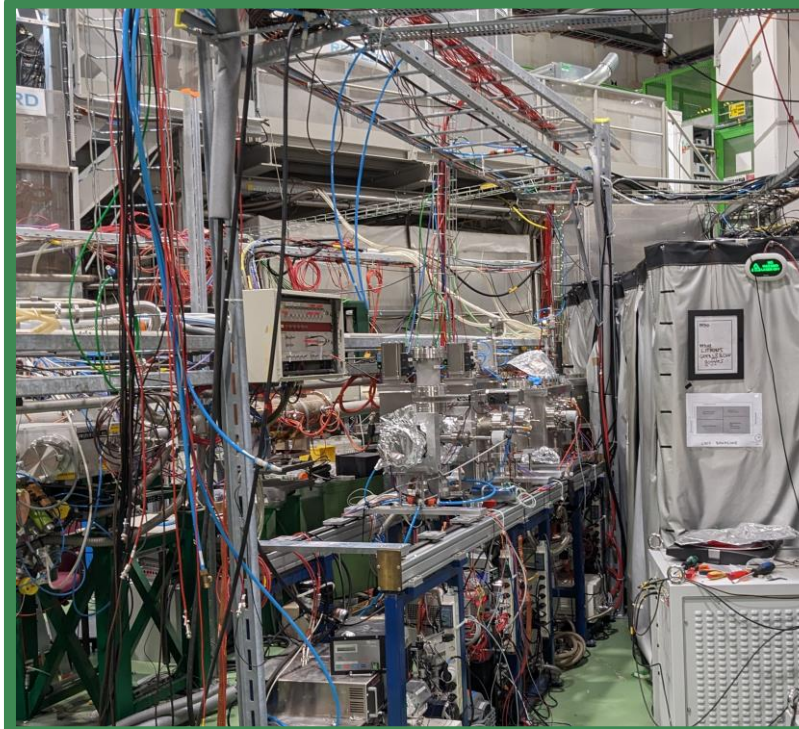
# 2023 CRIS upgrade: New End of the Beam Line

10

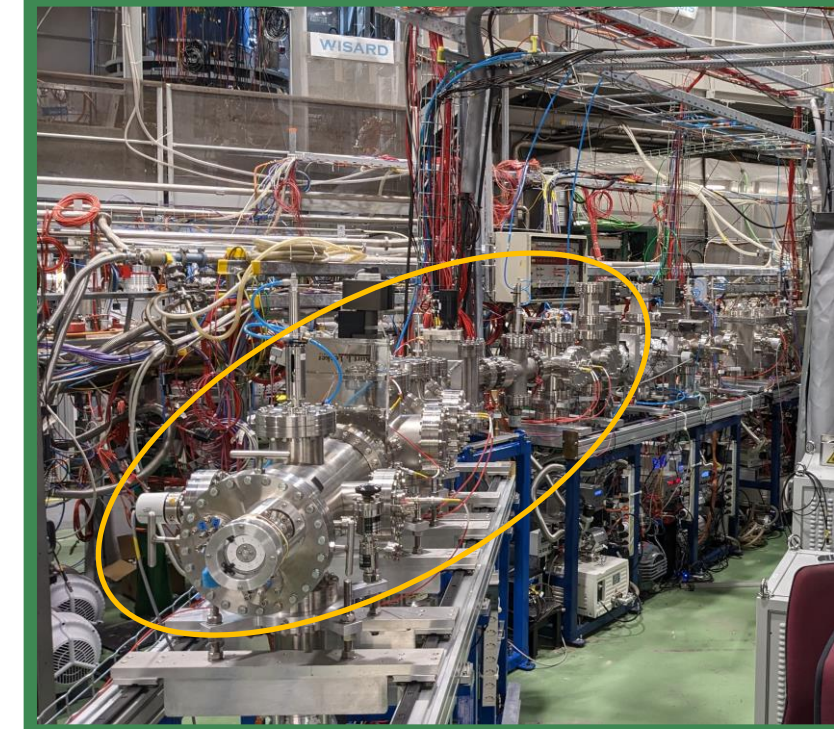
December 2022



January 2023



March 2023



## New end of the beam line:

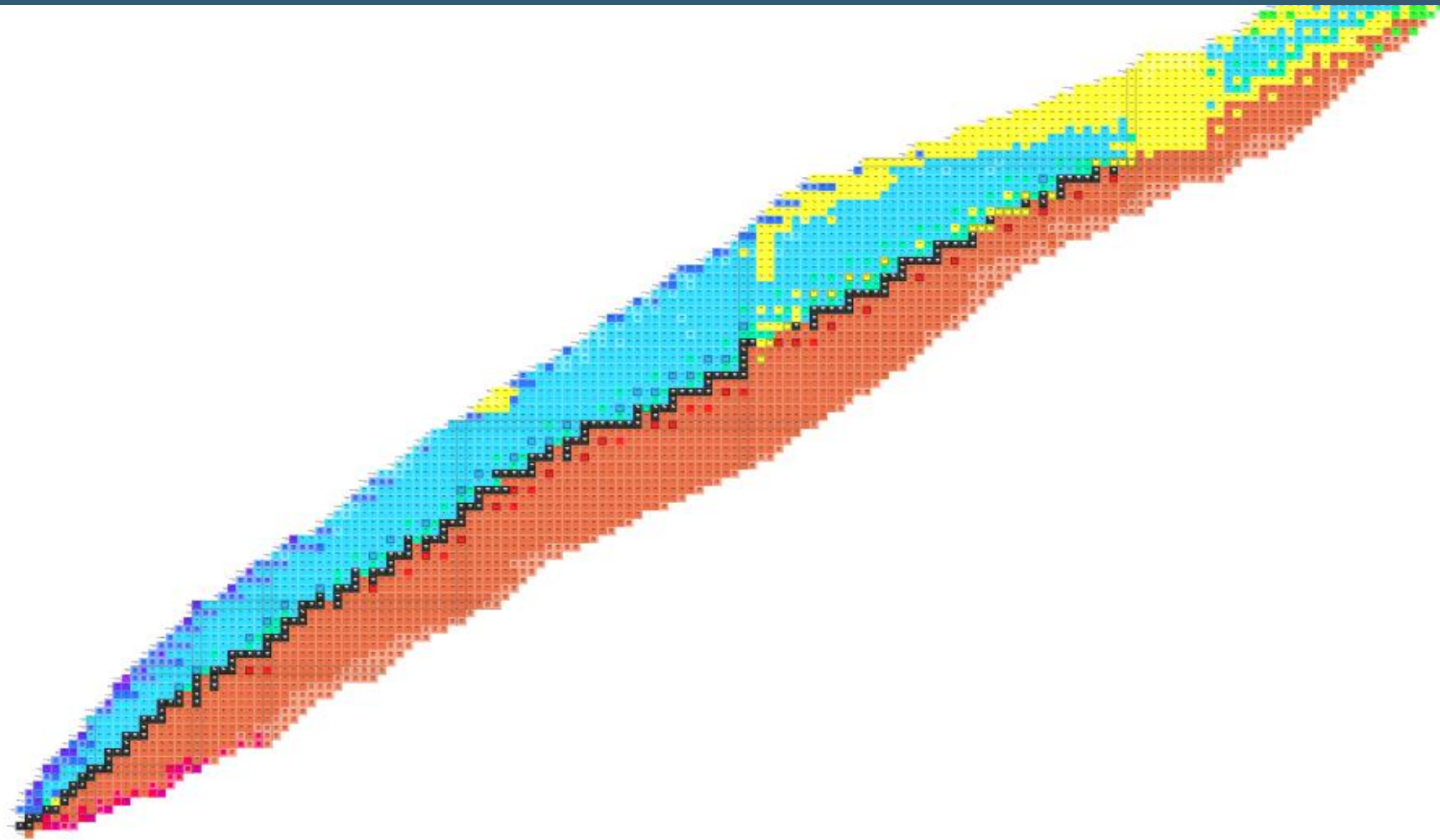
- New field ionization unit
- New bender
- New beam optics

- Allows Rydberg ionization scheme
- Beam transport efficiency toward ion detector and decay spectroscopy station improved from 30% to 100%
- Enable upgrade of the DSS toward a tape system

See talk of Yongchao Liu !

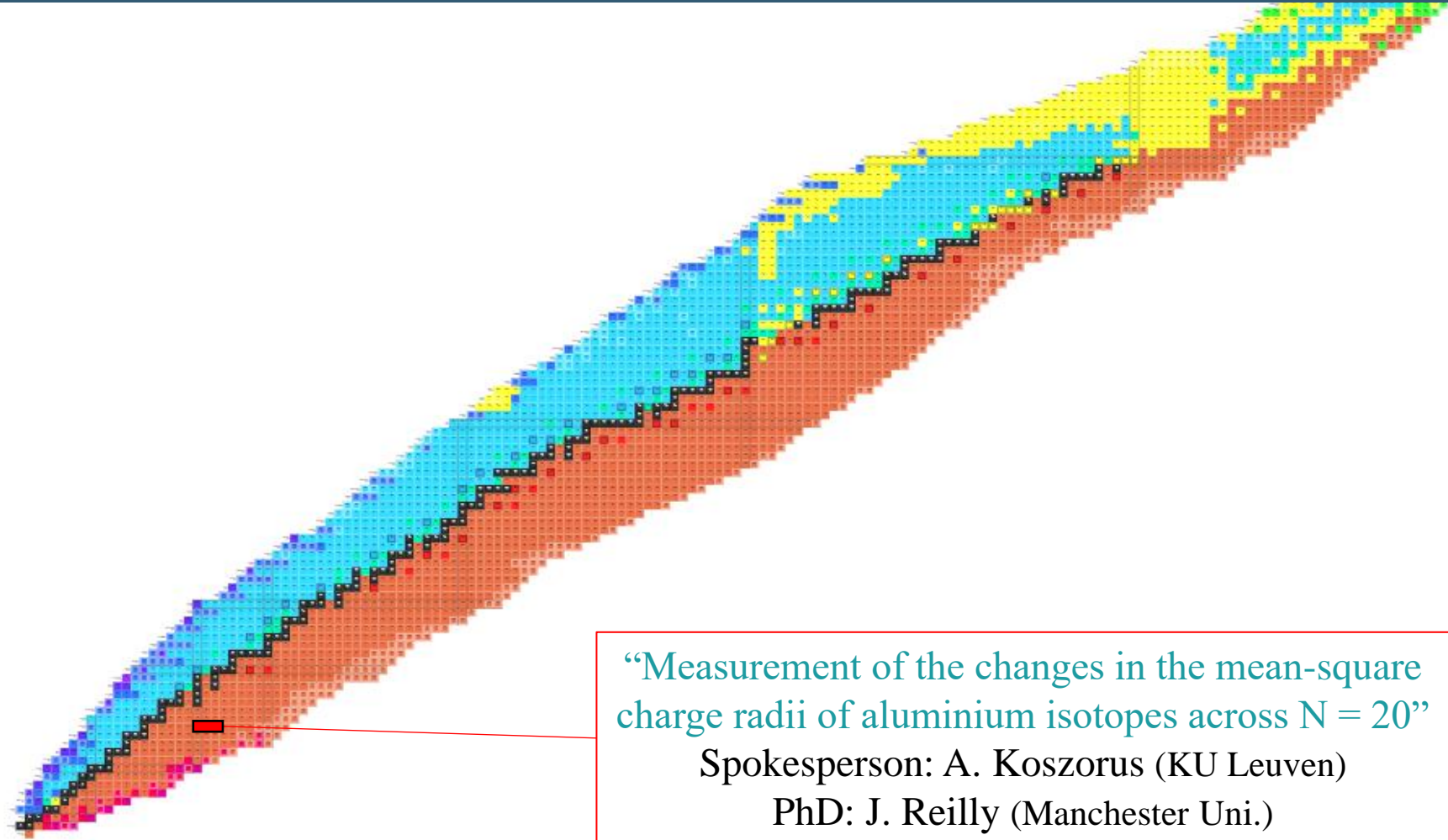


# The 2023 experimental campaign



	HRS schedule 2023																																																								
	April			May			June			July			August			September			October			November																																			
WK	14	15	16	17	18	19	20	21	22	23	24	25	26	27	28	29	30	31	32	33	34	35	36	37	38	39	40	41	42	43	44	45	46																								
MO	THC				17	24			15	22	29	#818 UC	8			#826 UC W	12	#828 UC Proto	5																																						
TU					#791 THC VDS																																																				
WE																																																									
TH																																																									
FR	G. Fri																																																								
SA																																																									
SU																																																									
	Time available for tests to CRIS																																																								
	TSD			TSD (days until Weekend)			COLLAPS			Ascension			CPIS			ISOLTRAP			if ready, pn scan yields			TS 30 h			#817 UC			#827 UC			IS712			IS700			IS714			IS733			IS682			IS733			IS663			CPIS			Fr		
	RILIS TI			RILIS AI			RaF			RaF			RILIS : Cr			K beams			RILIS: Tm			RILIS: Zn			Cs beams			SnS beam			SnS beam			K beams			RaF			RaF/Fr			ISOLDE Winter physics														

# The 2023 experimental campaign



“Measurement of the changes in the mean-square charge radii of aluminium isotopes across N = 20”

Spokesperson: A. Koszorus (KU Leuven)

PhD: J. Reilly (Manchester Uni.)

	April							May					June					July				August					September				October					November	
WK	14	15	16	17	18	19	20	21	22	23	24	25	26	27	28	29	30	31	32	33	34	35	36	37	38	39	40	41	42	43	44	45	46				
MO	THC				17	24		15	#791 THC VDS	Rb16 UC	B																										
TU																																					
WE																																					
TH																																					
FR	G. Fri																																				
SA																																					
SU																																					
Time available for tests to CRIS							TSD (days until Weekend)					ISOL TRAP					Ascension				CPIS					TS 30 h				ISOLTRAP					ISOLDE Winter physics		
TSD							CPIS					IS700					ISOLTRAP				IS712					IS712				IS714					RaF		
RILIS TI							RILIS AI					RILIS Cr					RaF				RILIS : Cr					K beams				RILIS: Tm					RILIS: Zn		
IS663							IS663					IS663					IS663				IS663					Cs beams				SnS beam					SnS beam		
IS663							IS663					IS663					IS663				IS663					K beams				RaF					RaF/Fr		

# The 2023 experimental campaign

14

# “Collinear resonance ionization spectroscopy of Chromium isotopes between N=28 and N=40”

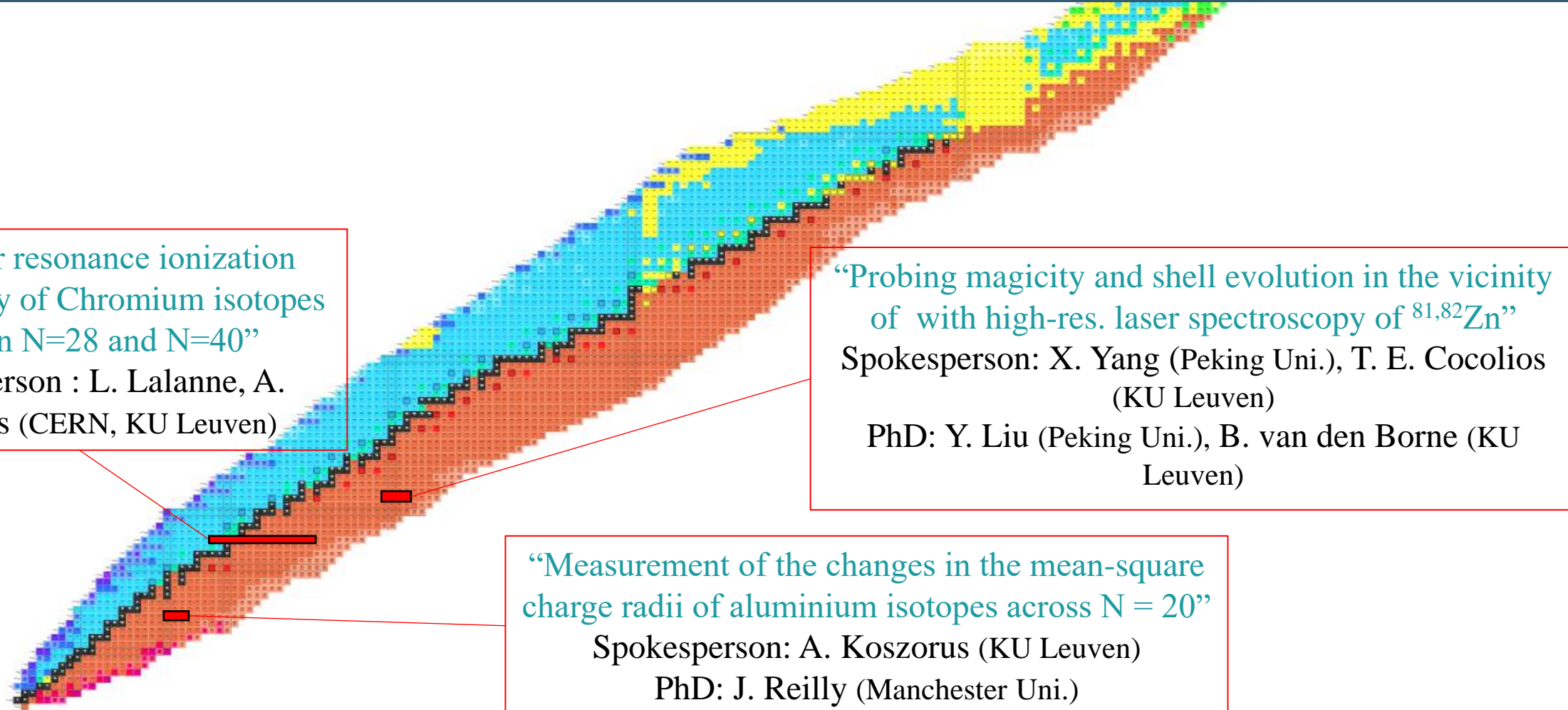
Spokesperson : L. Lalanne, A. Koszorus (CERN, KU Leuven)

# “Measurement of the changes in the mean-square charge radii of aluminium isotopes across N = 20”

Spokesperson: A. Koszorus (KU Leuven)  
PhD: J. Reilly (Manchester Uni.)

# The 2023 experimental campaign

15



# The 2023 experimental campaign

# “Rotational and hyperfine structure of RaF molecules”

Spokesperson: M. Athanasakis-Kaklamanakis (KU Leuven)  
CERN), S. Wilkins, R. Garzia-Riuz (MIT)  
PhD: Carlos Fajardo-Zambrano (KU Leuven)

# “Collinear resonance ionization spectroscopy of Chromium isotopes between N=28 and N=40”

Spokesperson : L. Lalanne, A. Koszorus (CERN, KU Leuven)

# “Probing magicity and shell evolution in the vicinity of $Z = 30$ with high-res. laser spectroscopy of $^{81,82}\text{Zn}$ ”

Spokesperson: X. Yang (Peking Uni.), T. E. Cocolios  
(KU Leuven)  
PhD: Y. Liu (Peking Uni.), B. van den Borne (KU  
Leuven)

# “Measurement of the changes in the mean-square charge radii of aluminium isotopes across N = 20”

Spokesperson: A. Koszorus (KU Leuven)

PhD: J. Reilly (Manchester Uni.)

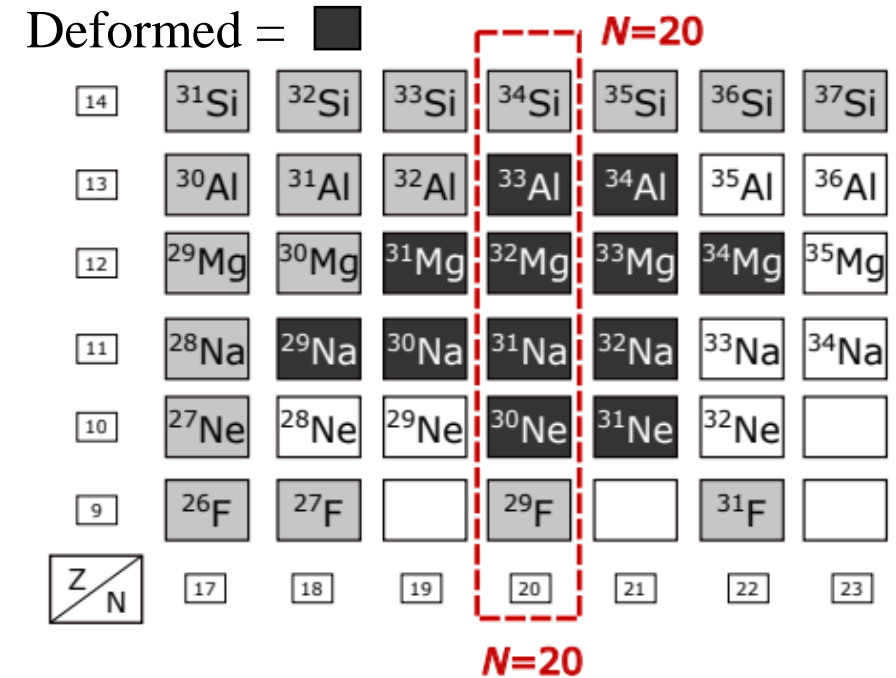




# Charge radii of Aluminium isotopes across $N = 20$

19

- $N=20$  Island of Inversion: Strongly mixed and deformed ground state configuration around  $^{32}\text{Mg}$
- $^{33}\text{Al}$  located between strongly deformed  $^{32}\text{Mg}$  and spherical  $^{34}\text{Si}$
- Evidence for  $^{33}\text{Al}$  g.s. deformation from quadrupole moment <sup>(1)</sup> - Transition into the Island of inversion?

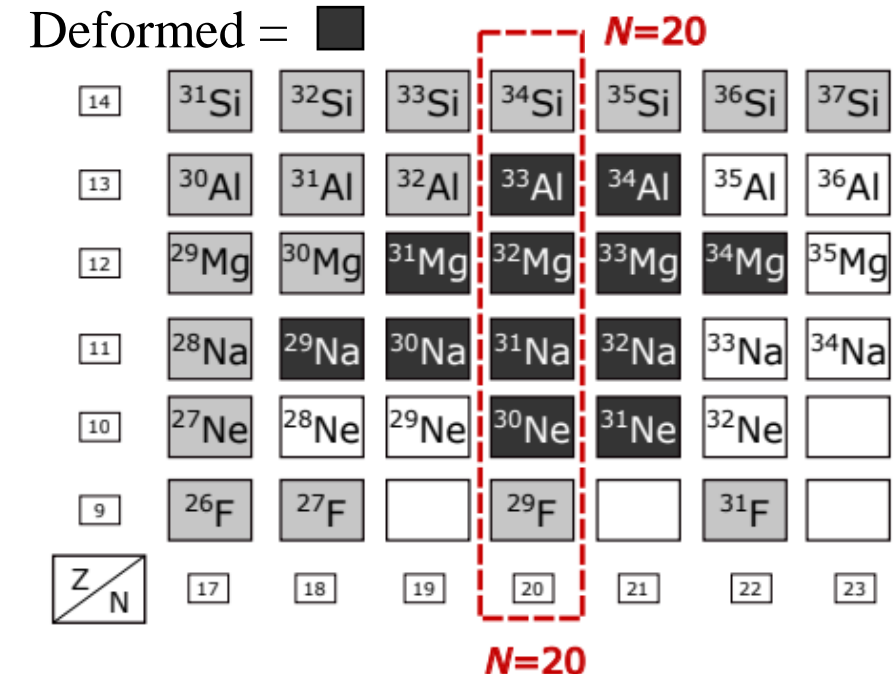
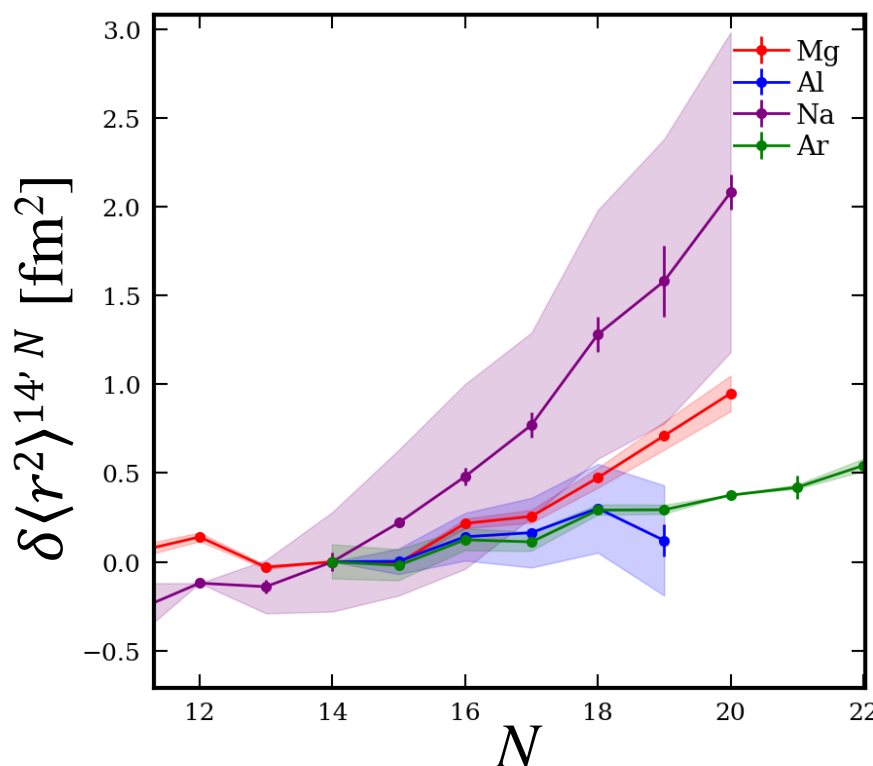


<sup>(1)</sup> Heylen et al., PHYSICAL REVIEW C **94**, 034312 (2016)

# Charge radii of Aluminium isotopes across $N = 20$

20

- $N=20$  Island of Inversion: Strongly mixed and deformed ground state configuration around  $^{32}\text{Mg}$
- $^{33}\text{Al}$  located between strongly deformed  $^{32}\text{Mg}$  and spherical  $^{34}\text{Si}$
- Evidence for  $^{33}\text{Al}$  g.s. deformation from quadrupole moment <sup>(1)</sup> - Transition into the Island of inversion?



- Large increase in charge radii towards the  $N = 20$  shell closure is observed for **Na** and **Mg**
- Previous measurements of **Al** radii display an unexpected decrease in  $\delta\langle r^2 \rangle$  between  $^{31}\text{Al}$  and  $^{32}\text{Al}$  <sup>(2)</sup>

<sup>(1)</sup> Heylen et al., PHYSICAL REVIEW C **94**, 034312 (2016)

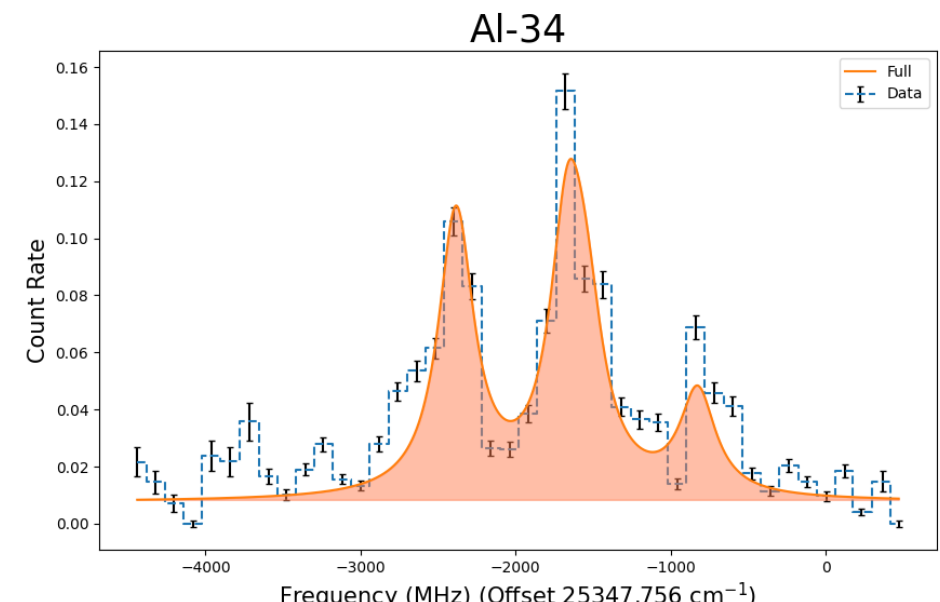
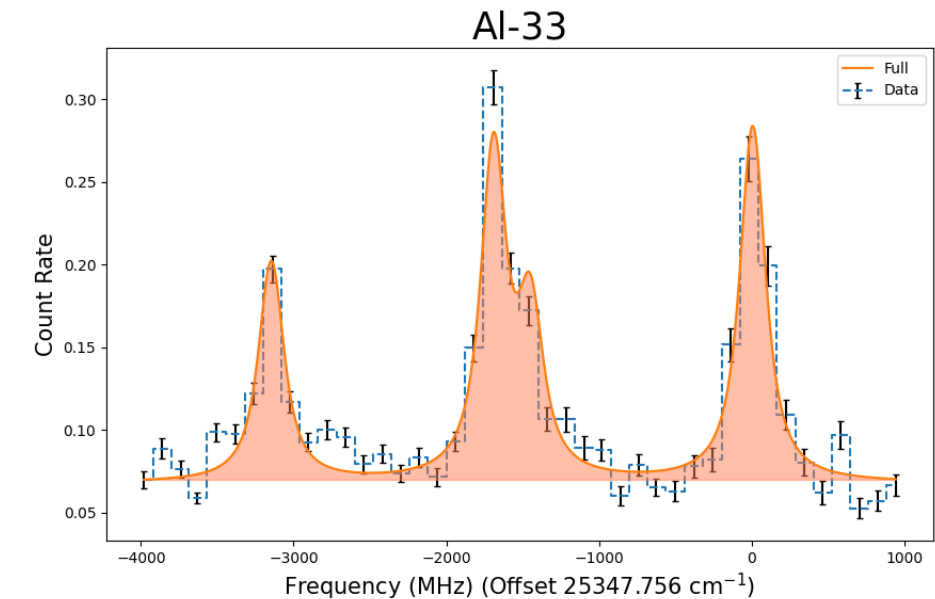
<sup>(2)</sup> Heylen et al., PHYSICAL REVIEW C **103**, 014318 (2021)

# Charge radii of Aluminium isotopes across N = 20

21

- Two runs: 2022 ( $^{27-32}\text{Al}$ ) and 2023 ( $^{33-34}\text{Al}$ )
- First laser spectroscopy measurement of Al across N=20
- Ongoing analysis to extract radii

Analysis and plots from Jordan Reilly



# The 2023 experimental campaign

22

“Rotational and hyperfine structure of RaF molecules”

Spokesperson: M. Athanasakis-Kaklamakanis (KU Leuven,  
CERN), S. Wilkins, R. Garzia-Riuz (MIT)  
PhD: Carlos Fajardo-Zambrano (KU Leuven)

“Collinear resonance ionization  
spectroscopy of Chromium isotopes  
between N=28 and N=40”

Spokesperson : L. Lalanne, A.  
Koszorus (CERN, KU Leuven)

“Probing mag See talk of Yongchao Liu !  
and shell evolution in the vicinity  
of with high-precision spectroscopy of  $^{81,82}\text{Zn}$ ”

Spokesperson: X. Yang (Peking Uni.), T. E. Cocolios  
(KU Leuven), Yongchao Liu (Peking Uni.), D. Borne (KU  
Leuven)

“Measurement of the changes in the mean-square  
charge radii of aluminium isotopes across N = 20”

Spokesperson: A. Koszorus (KU Leuven)  
PhD: J. Reilly (Manchester Uni.)

	April				May				June				July				August				September				October				November				
WK	14	15	16	17	18	19	20	21	22	23	24	25	26	27	28	29	30	31	32	33	34	35	36	37	38	39	40	41	42	43	44	45	46
MO	THC	3			10																												
TU																																	
WE																																	
TH																																	
FR	G. Fri																																
SA																																	
SU																																	
	Time available for tests to CRIS				#791 THC VDS				ISOL TRAP				Ascension				#817 UC				#827 UC				#836 UC W				#837 UC + S				
	TSD (days until Weekend)				RILIS TI				RILIS AI				RILIS : Cr				RaF				RILIS : Cr				RILIS : Tm				RILIS : Zn				
	ISOLDE				ISOLTRAP				CPIS				ISOLTRAP				ISOLTRAP				CPIS				ISOLTRAP				ISOLTRAP				
	K beams				K beams				K beams				K beams				Cs beams				SnS beam				SnS beam				K beams				
	RaF				RaF				RaF				RaF				RaF				RaF				RaF				RaF/Fr				
	ISOLDE Winter physics																																

HRS schedule 2023

# The N=40 Island of Inversion and the Cr isotopes

23

The Cr isotopes:

- Half filled  $f_{7/2}$  → strongest  $p$ - $n$  collectivity
- Mass : gradual increase of collectivity and deformation from  $N=34$  onward <sup>(1)</sup>
- Radii of Mn ( $Z=25$ ): suggested onset of deformation around  $N=35$  <sup>(2)</sup>
- $^{64}\text{Cr}$  is the predicted center of the  $N=40$  Island of Inv.
- No firm assignment of g.s. spins
- No radii or moments known outside stability

$Z = 28$

$^{56}\text{Ni}$ $\beta^+$	$^{57}\text{Ni}$ $\beta^+$	$^{58}\text{Ni}$ $2\beta^+$	$^{59}\text{Ni}$ $\beta^+$	$^{60}\text{Ni}$ Stable	$^{61}\text{Ni}$ Stable	$^{62}\text{Ni}$ Stable	$^{63}\text{Ni}$ $\beta^-$	$^{64}\text{Ni}$ Stable	$^{65}\text{Ni}$ $\beta^-$	$^{66}\text{Ni}$ $\beta^-$	$^{67}\text{Ni}$ $\beta^-$	$^{68}\text{Ni}$ $\beta^-$
$^{55}\text{Co}$ $\beta^+$	$^{56}\text{Co}$ $\beta^+$	$^{57}\text{Co}$ e- capture	$^{58}\text{Co}$ $\beta^+$	$^{59}\text{Co}$ Stable	$^{60}\text{Co}$ $\beta^-$	$^{61}\text{Co}$ $\beta^-$	$^{62}\text{Co}$ $\beta^-$	$^{63}\text{Co}$ $\beta^-$	$^{64}\text{Co}$ $\beta^-$	$^{65}\text{Co}$ $\beta^-$	$^{66}\text{Co}$ $\beta^-$	$^{67}\text{Co}$ $\beta^-$
$^{54}\text{Fe}$ $2\beta^+$	$^{55}\text{Fe}$ e- capture	$^{56}\text{Fe}$ Stable	$^{57}\text{Fe}$ Stable	$^{58}\text{Fe}$ Stable	$^{59}\text{Fe}$ $\beta^-$	$^{60}\text{Fe}$ $\beta^-$	$^{61}\text{Fe}$ $\beta^-$	$^{62}\text{Fe}$ $\beta^-$	$^{63}\text{Fe}$ $\beta^-$	$^{64}\text{Fe}$ $\beta^-$	$^{65}\text{Fe}$ $\beta^-$	$^{66}\text{Fe}$ $\beta^-$
$^{53}\text{Mn}$ e- capture	$^{54}\text{Mn}$ e- capture	$^{55}\text{Mn}$ Stable	$^{56}\text{Mn}$ $\beta^-$	$^{57}\text{Mn}$ $\beta^-$	$^{58}\text{Mn}$ $\beta^-$	$^{59}\text{Mn}$ $\beta^-$	$^{60}\text{Mn}$ $\beta^-$	$^{61}\text{Mn}$ $\beta^-$	$^{62}\text{Mn}$ $\beta^-$	$^{63}\text{Mn}$ $\beta^-$	$^{64}\text{Mn}$ $\beta^-$	$^{65}\text{Mn}$ $\beta^-$
$^{52}\text{Cr}$ Stable	$^{53}\text{Cr}$ Stable	$^{54}\text{Cr}$ Stable	$^{55}\text{Cr}$ $\beta^-$	$^{56}\text{Cr}$ $\beta^-$	$^{57}\text{Cr}$ $\beta^-$	$^{58}\text{Cr}$ $\beta^-$	$^{59}\text{Cr}$ $\beta^-$	$^{60}\text{Cr}$ $\beta^-$	$^{61}\text{Cr}$ $\beta^-$	$^{62}\text{Cr}$ $\beta^-$	$^{63}\text{Cr}$ $\beta^-$	$^{64}\text{Cr}$ $\beta^-$

$Z = 24$

$^{51}\text{V}$ Stable	$^{52}\text{V}$ $\beta^-$	$^{53}\text{V}$ $\beta^-$	$^{54}\text{V}$ $\beta^-$	$^{55}\text{V}$ $\beta^-$	$^{56}\text{V}$ $\beta^-$	$^{57}\text{V}$ $\beta^-$	$^{58}\text{V}$ $\beta^-$	$^{59}\text{V}$ $\beta^-$	$^{60}\text{V}$ $\beta^-$	$^{61}\text{V}$ $\beta^-$	$^{62}\text{V}$ $\beta^-$	$^{63}\text{V}$ $\beta^-$
$^{50}\text{Ti}$ Stable	$^{51}\text{Ti}$ $\beta^-$	$^{52}\text{Ti}$ $\beta^-$	$^{53}\text{Ti}$ $\beta^-$	$^{54}\text{Ti}$ $\beta^-$	$^{55}\text{Ti}$ $\beta^-$	$^{56}\text{Ti}$ $\beta^-$	$^{57}\text{Ti}$ $\beta^-$	$^{58}\text{Ti}$ $\beta^-$	$^{59}\text{Ti}$ $\beta^-$	$^{60}\text{Ti}$ $\beta^-$	$^{61}\text{Ti}$ $\beta^-$	$^{62}\text{Ti}$ $\beta^-$
$^{49}\text{Sc}$ $\beta^-$	$^{50}\text{Sc}$ $\beta^-$	$^{51}\text{Sc}$ $\beta^-$	$^{52}\text{Sc}$ $\beta^-$	$^{53}\text{Sc}$ $\beta^-$	$^{54}\text{Sc}$ $\beta^-$	$^{55}\text{Sc}$ $\beta^-$	$^{56}\text{Sc}$ $\beta^-$	$^{57}\text{Sc}$ $\beta^-$	$^{58}\text{Sc}$ $\beta^-$	$^{59}\text{Sc}$ $\beta^-$	$^{60}\text{Sc}$ $\beta^-$	$^{61}\text{Sc}$ $\beta^-$
$^{48}\text{Ca}$ $2\beta^-$	$^{49}\text{Ca}$ $\beta^-$	$^{50}\text{Ca}$ $\beta^-$	$^{51}\text{Ca}$ $\beta^-$	$^{52}\text{Ca}$ $\beta^-$	$^{53}\text{Ca}$ $\beta^-$	$^{54}\text{Ca}$ $\beta^-$	$^{55}\text{Ca}$ $\beta^-$	$^{56}\text{Ca}$ $\beta^-$	$^{57}\text{Ca}$ $\beta^-$	$^{58}\text{Ca}$ $\beta^-$	$^{59}\text{Ca}$ $\beta^-$	$^{60}\text{Ca}$ $\beta^-$

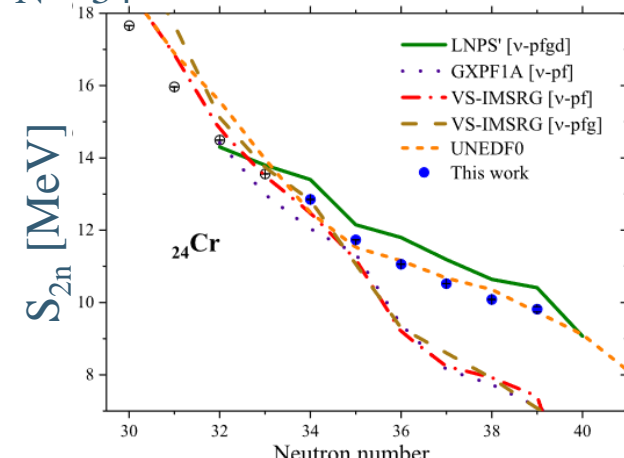
$Z = 20$

$N = 28$

$N = 32$

$N = 34$

$N = 40$



<sup>(1)</sup> M. Mougeot *et al.*, PRL **120**, 232501 (2018)

<sup>(2)</sup> H. Heylen *et al.*, PRC **94**, 054321 (2016)

# The N=40 Island of Inversion and the Cr isotopes

The Cr isotopes:

- Half filled  $f_{7/2}$  → strongest  $p$ - $n$  collectivity
- Mass : gradual increase of collectivity and deformation from  $N=34$  onward <sup>(1)</sup>
- Radii of Mn ( $Z=25$ ): suggested onset of deformation around  $N=35$  <sup>(2)</sup>
- $^{64}\text{Cr}$  is the predicted center of the  $N=40$  Island of Inv.
- No firm assignment of g.s. spins
- No radii or moments known outside stability

$Z = 28$

$^{56}\text{Ni}$ $\beta^+$	$^{57}\text{Ni}$ $\beta^+$	$^{58}\text{Ni}$ $2\beta^+$	$^{59}\text{Ni}$ $\beta^+$	$^{60}\text{Ni}$ Stable	$^{61}\text{Ni}$ Stable	$^{62}\text{Ni}$ Stable	$^{63}\text{Ni}$ $\beta^-$	$^{64}\text{Ni}$ Stable	$^{65}\text{Ni}$ $\beta^-$	$^{66}\text{Ni}$ $\beta^-$	$^{67}\text{Ni}$ $\beta^-$	$^{68}\text{Ni}$ $\beta^-$
$^{55}\text{Co}$ $\beta^+$	$^{56}\text{Co}$ $\beta^+$	$^{57}\text{Co}$ e- capture	$^{58}\text{Co}$ $\beta^+$	$^{59}\text{Co}$ Stable	$^{60}\text{Co}$ $\beta^-$	$^{61}\text{Co}$ $\beta^-$	$^{62}\text{Co}$ $\beta^-$	$^{63}\text{Co}$ $\beta^-$	$^{64}\text{Co}$ $\beta^-$	$^{65}\text{Co}$ $\beta^-$	$^{66}\text{Co}$ $\beta^-$	$^{67}\text{Co}$ $\beta^-$
$^{54}\text{Fe}$ $2\beta^+$	$^{55}\text{Fe}$ e- capture	$^{56}\text{Fe}$ Stable	$^{57}\text{Fe}$ Stable	$^{58}\text{Fe}$ Stable	$^{59}\text{Fe}$ $\beta^-$	$^{60}\text{Fe}$ $\beta^-$	$^{61}\text{Fe}$ $\beta^-$	$^{62}\text{Fe}$ $\beta^-$	$^{63}\text{Fe}$ $\beta^-$	$^{64}\text{Fe}$ $\beta^-$	$^{65}\text{Fe}$ $\beta^-$	$^{66}\text{Fe}$ $\beta^-$
$^{53}\text{Mn}$ e- capture	$^{54}\text{Mn}$ e- capture	$^{55}\text{Mn}$ Stable	$^{56}\text{Mn}$ $\beta^-$	$^{57}\text{Mn}$ $\beta^-$	$^{58}\text{Mn}$ $\beta^-$	$^{59}\text{Mn}$ $\beta^-$	$^{60}\text{Mn}$ $\beta^-$	$^{61}\text{Mn}$ $\beta^-$	$^{62}\text{Mn}$ $\beta^-$	$^{63}\text{Mn}$ $\beta^-$	$^{64}\text{Mn}$ $\beta^-$	$^{65}\text{Mn}$ $\beta^-$
$^{52}\text{Cr}$ Stable	$^{53}\text{Cr}$ Stable	$^{54}\text{Cr}$ Stable	$^{55}\text{Cr}$ $\beta^-$	$^{56}\text{Cr}$ $\beta^-$	$^{57}\text{Cr}$ $\beta^-$	$^{58}\text{Cr}$ $\beta^-$	$^{59}\text{Cr}$ $\beta^-$	$^{60}\text{Cr}$ $\beta^-$	$^{61}\text{Cr}$ $\beta^-$	$^{62}\text{Cr}$ $\beta^-$	$^{63}\text{Cr}$ $\beta^-$	$^{64}\text{Cr}$ $\beta^-$

$Z = 24$

$^{51}\text{V}$ Stable	$^{52}\text{V}$ $\beta^-$	$^{53}\text{V}$ $\beta^-$	$^{54}\text{V}$ $\beta^-$	$^{55}\text{V}$ $\beta^-$	$^{56}\text{V}$ $\beta^-$	$^{57}\text{V}$ $\beta^-$	$^{58}\text{V}$ $\beta^-$	$^{59}\text{V}$ $\beta^-$	$^{60}\text{V}$ $\beta^-$	$^{61}\text{V}$ $\beta^-$	$^{62}\text{V}$ $\beta^-$	$^{63}\text{V}$ $\beta^-$
$^{50}\text{Ti}$ Stable	$^{51}\text{Ti}$ $\beta^-$	$^{52}\text{Ti}$ $\beta^-$	$^{53}\text{Ti}$ $\beta^-$	$^{54}\text{Ti}$ $\beta^-$	$^{55}\text{Ti}$ $\beta^-$	$^{56}\text{Ti}$ $\beta^-$	$^{57}\text{Ti}$ $\beta^-$	$^{58}\text{Ti}$ $\beta^-$	$^{59}\text{Ti}$ $\beta^-$	$^{60}\text{Ti}$ $\beta^-$	$^{61}\text{Ti}$ $\beta^-$	$^{62}\text{Ti}$ $\beta^-$
$^{49}\text{Sc}$ $\beta^-$	$^{50}\text{Sc}$ $\beta^-$	$^{51}\text{Sc}$ $\beta^-$	$^{52}\text{Sc}$ $\beta^-$	$^{53}\text{Sc}$ $\beta^-$	$^{54}\text{Sc}$ $\beta^-$	$^{55}\text{Sc}$ $\beta^-$	$^{56}\text{Sc}$ $\beta^-$	$^{57}\text{Sc}$ $\beta^-$	$^{58}\text{Sc}$ $\beta^-$	$^{59}\text{Sc}$ $\beta^-$	$^{60}\text{Sc}$ $\beta^-$	$^{61}\text{Sc}$ $\beta^-$
$^{48}\text{Ca}$ $2\beta^-$	$^{49}\text{Ca}$ $\beta^-$	$^{50}\text{Ca}$ $\beta^-$	$^{51}\text{Ca}$ $\beta^-$	$^{52}\text{Ca}$ $\beta^-$	$^{53}\text{Ca}$ $\beta^-$	$^{54}\text{Ca}$ $\beta^-$	$^{55}\text{Ca}$ $\beta^-$	$^{56}\text{Ca}$ $\beta^-$	$^{57}\text{Ca}$ $\beta^-$	$^{58}\text{Ca}$ $\beta^-$	$^{59}\text{Ca}$ $\beta^-$	$^{60}\text{Ca}$ $\beta^-$

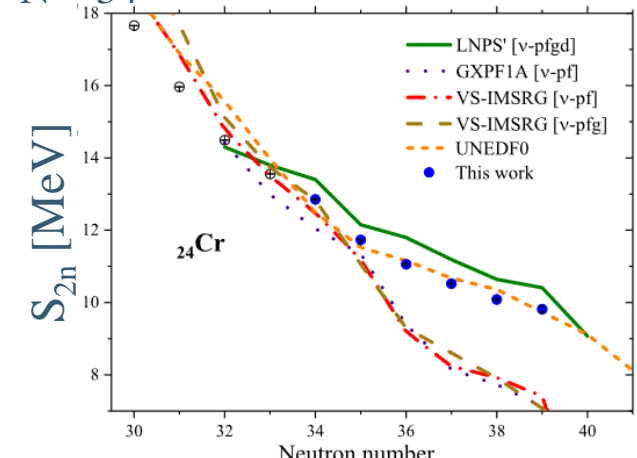
$Z = 20$

$N = 28$

$N = 32$

$N = 34$

$N = 40$



<sup>(1)</sup> M. Mougeot *et al.*, PRL **120**, 232501 (2018)

<sup>(2)</sup> H. Heylen *et al.*, PRC **94**, 054321 (2016)

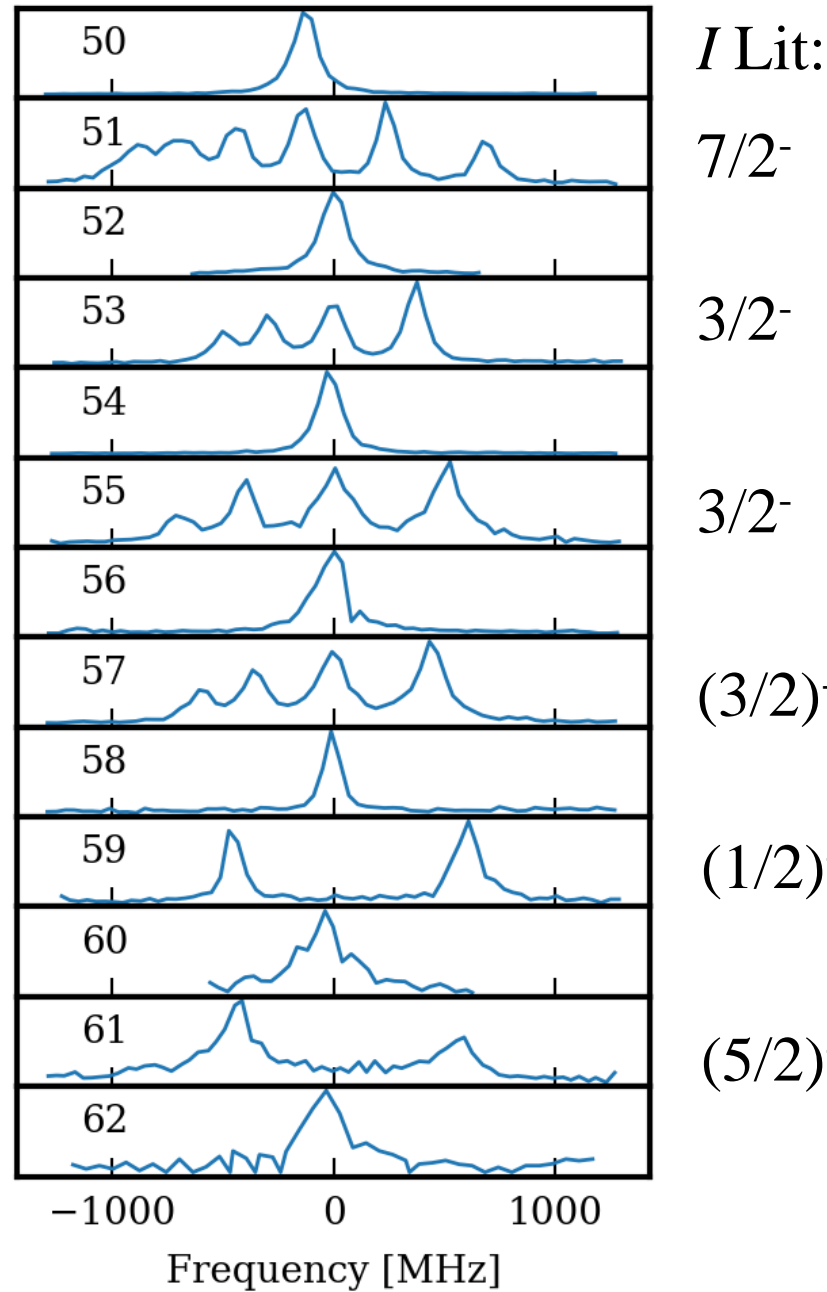
→ Laser RIS scheme developed by RILIS

Goals:

- Firm spin assignment outside stability
- Better understand the structure of the odd- $A$  Cr ground states
- Investigate the structural changes along the chain and the formation of the  $N=40$  IoI

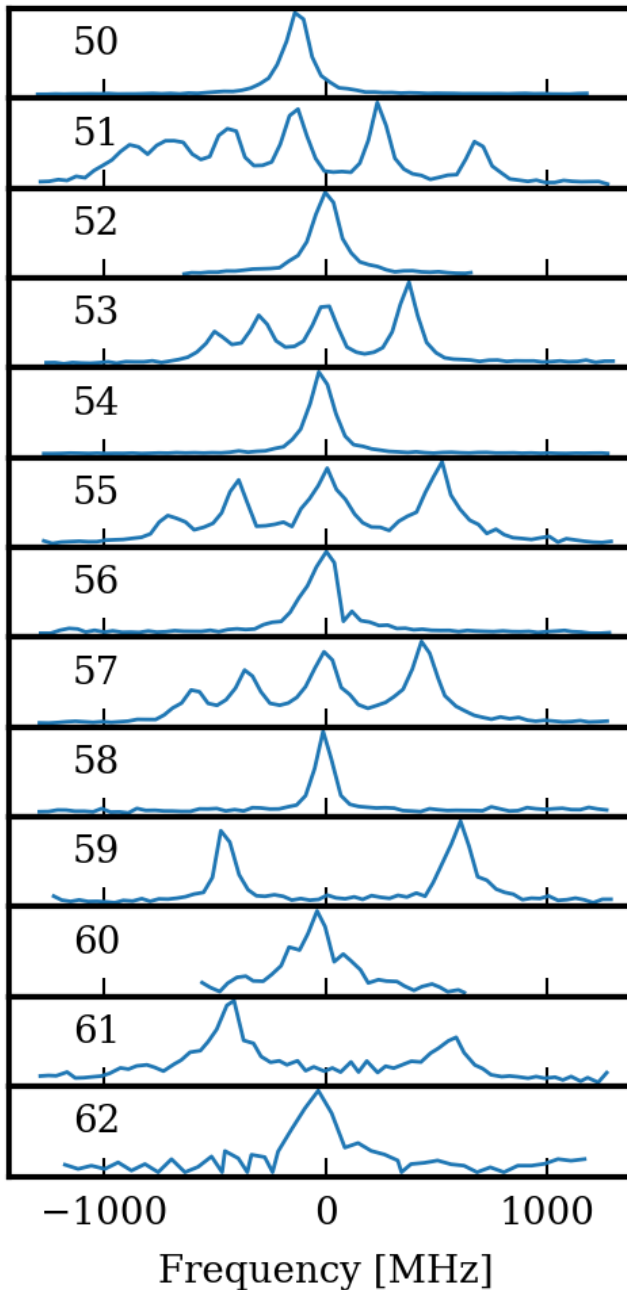
# Cr Results: spins of odd-*A* Cr isotopes

25



# Cr Results: spins of odd-*A* Cr isotopes

26



*I* Lit:    *I* CRIS:

7/2<sup>-</sup>      7/2<sup>-</sup>

3/2<sup>-</sup>      3/2<sup>-</sup>

3/2<sup>-</sup>      3/2<sup>-</sup>

(3/2)<sup>-</sup>      3/2<sup>-</sup>

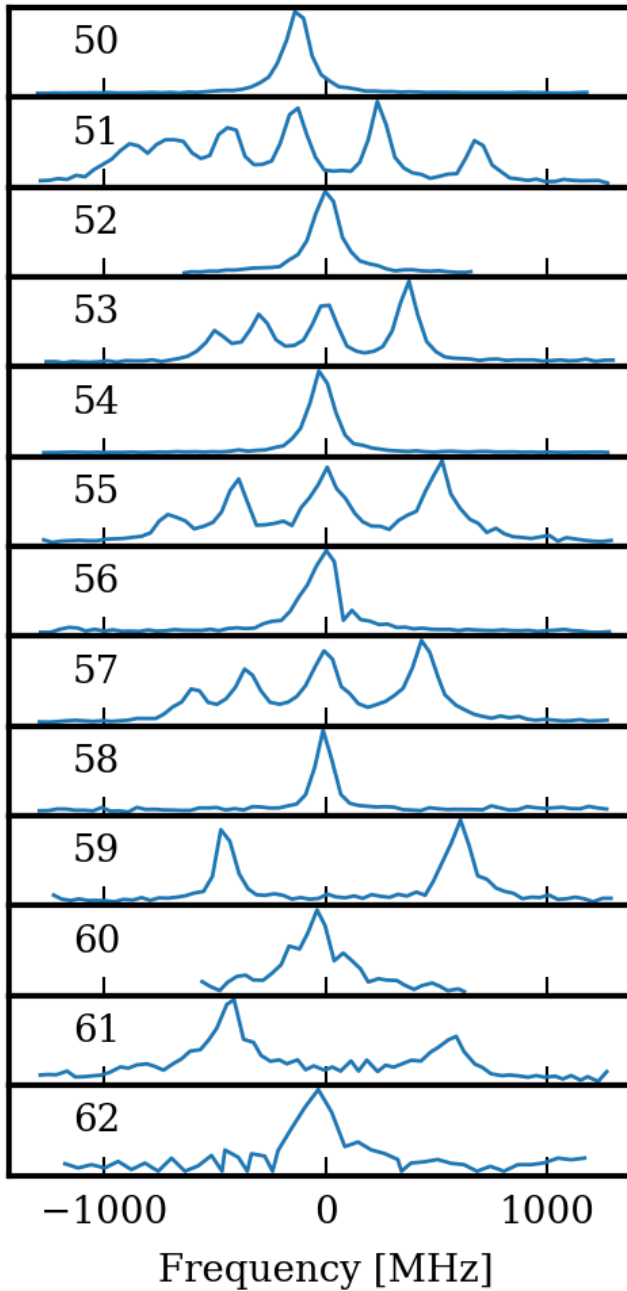
(1/2)<sup>-</sup>      1/2<sup>-</sup>

(5/2)<sup>-</sup>      1/2<sup>-</sup>

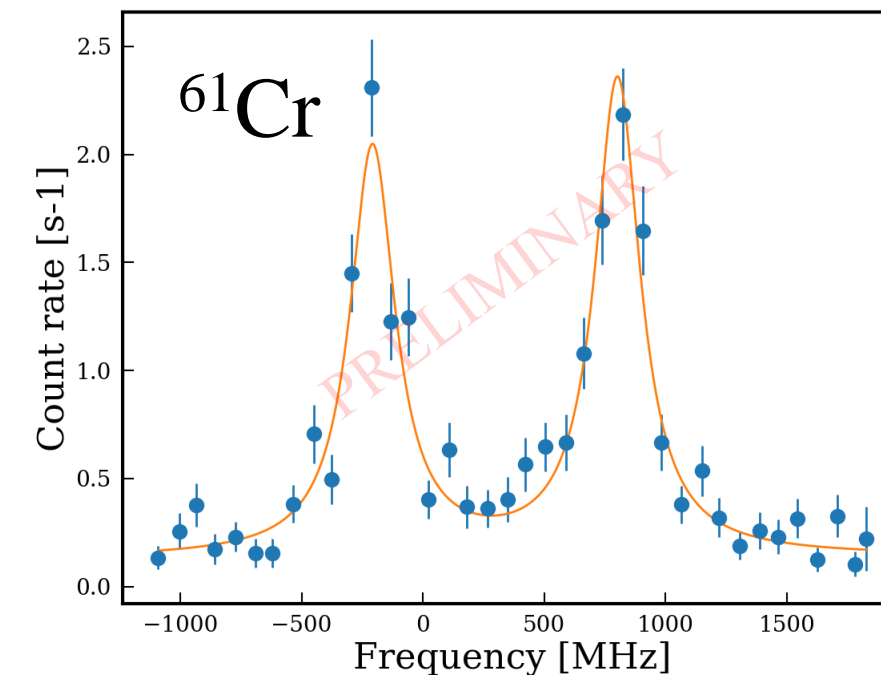
- First firm spin assignment of  $^{57,59,61}\text{Cr}$
- $^{57}\text{Cr}$  and  $^{59}\text{Cr}$  spins confirmed to be 3/2 and 1/2, respectively

# Cr Results: spins of odd- $A$ Cr isotopes

27



$I$ Lit:	$I$ CRIS:
7/2 $^-$	7/2 $^-$
5/2	3/2 $^-$
5/2	3/2 $^-$
5/4	3/2 $^-$
5/5	3/2 $^-$
5/6	3/2 $^-$
5/7	3/2 $^-$
5/8	3/2 $^-$
(3/2) $^-$	3/2 $^-$
5/9	1/2 $^-$
6/0	1/2 $^-$
6/1	1/2 $^-$
6/2	1/2 $^-$



- First firm spin assignment of  $^{57,59,61}\text{Cr}$
  - $^{57}\text{Cr}$  and  $^{59}\text{Cr}$  spins confirmed to be 3/2 and 1/2, respectively
  - $^{61}\text{Cr}$  found to be 1/2 , in disagreement with 5/2 assignment from beta decay experiments
- Large consequences on the interpretation of beta decay data and on the  $^{61}\text{Cr}$  and  $^{61}\text{Mn}$  level schemes

# Results: g factors of odd-*A* Cr isotopes

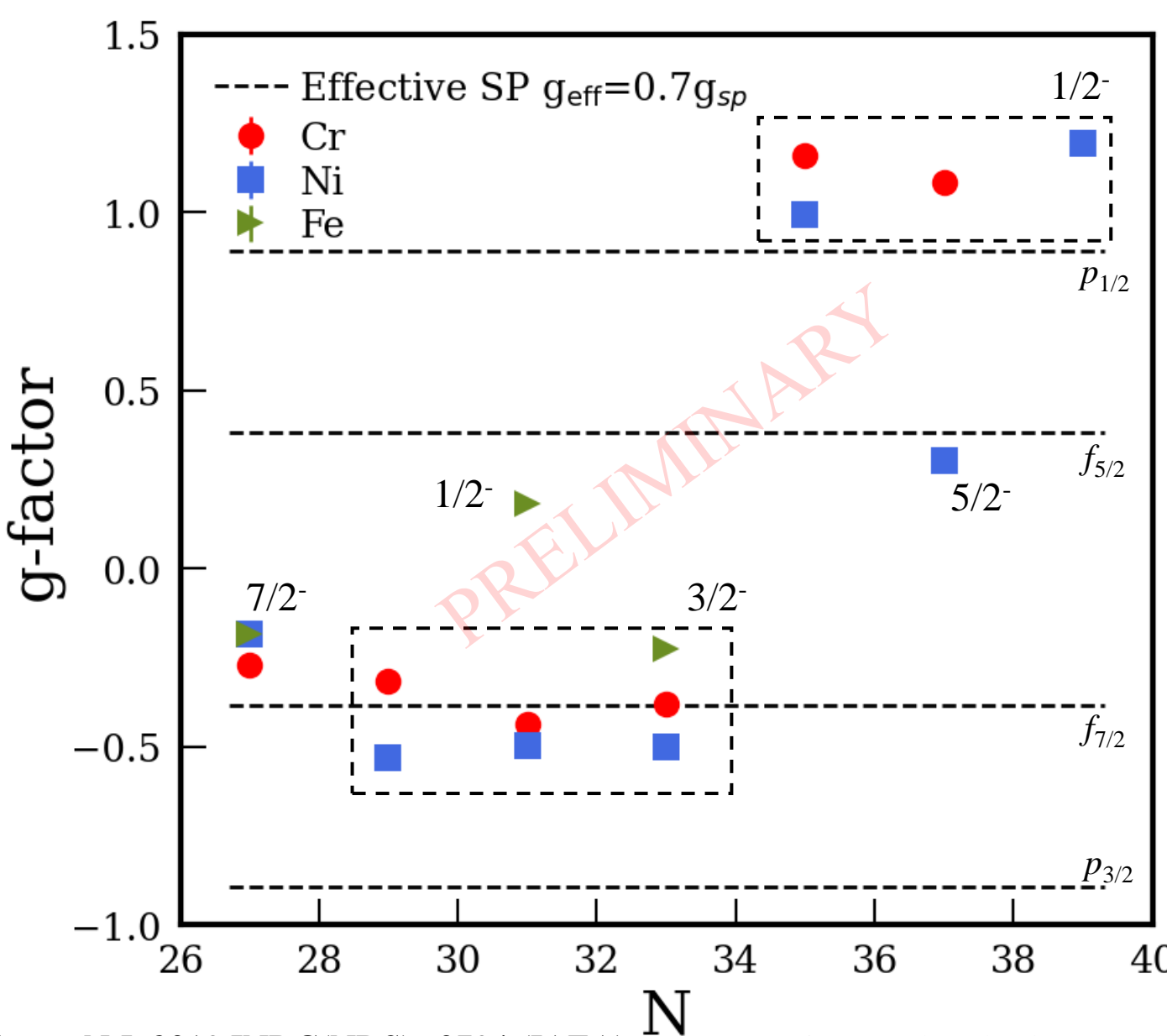
28

g-factor : 
$$g = \frac{\mu}{I\mu_N}$$

→ Very sensitive to which orbitals are occupied by the valence particles

# Results: g factors of odd-*A* Cr isotopes

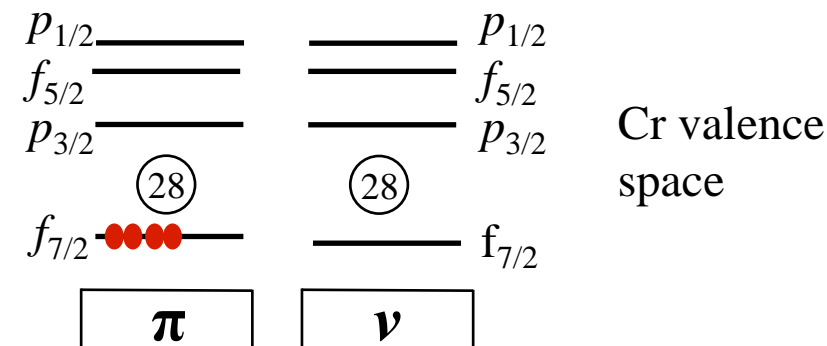
29



g-factor :

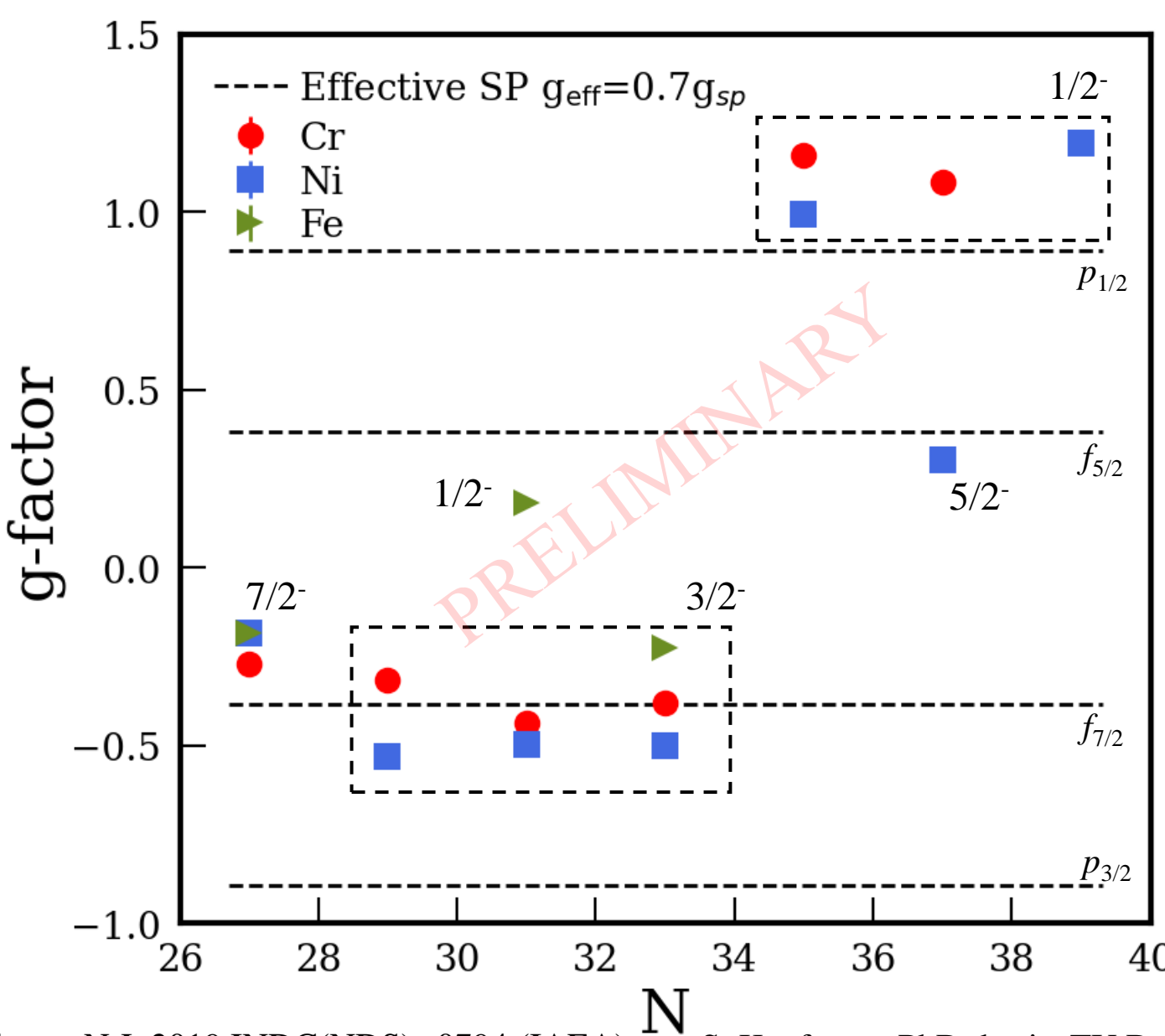
$$g = \frac{\mu}{I\mu_N}$$

→ Very sensitive to which orbitals are occupied by the valence particles



# Results: g factors of odd-*A* Cr isotopes

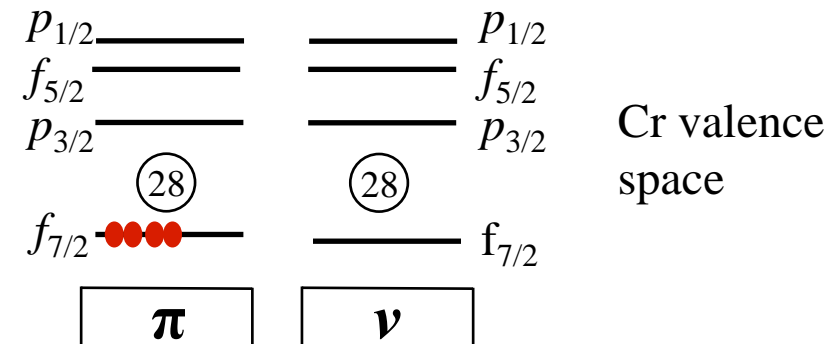
30



g-factor :

$$g = \frac{\mu}{I\mu_N}$$

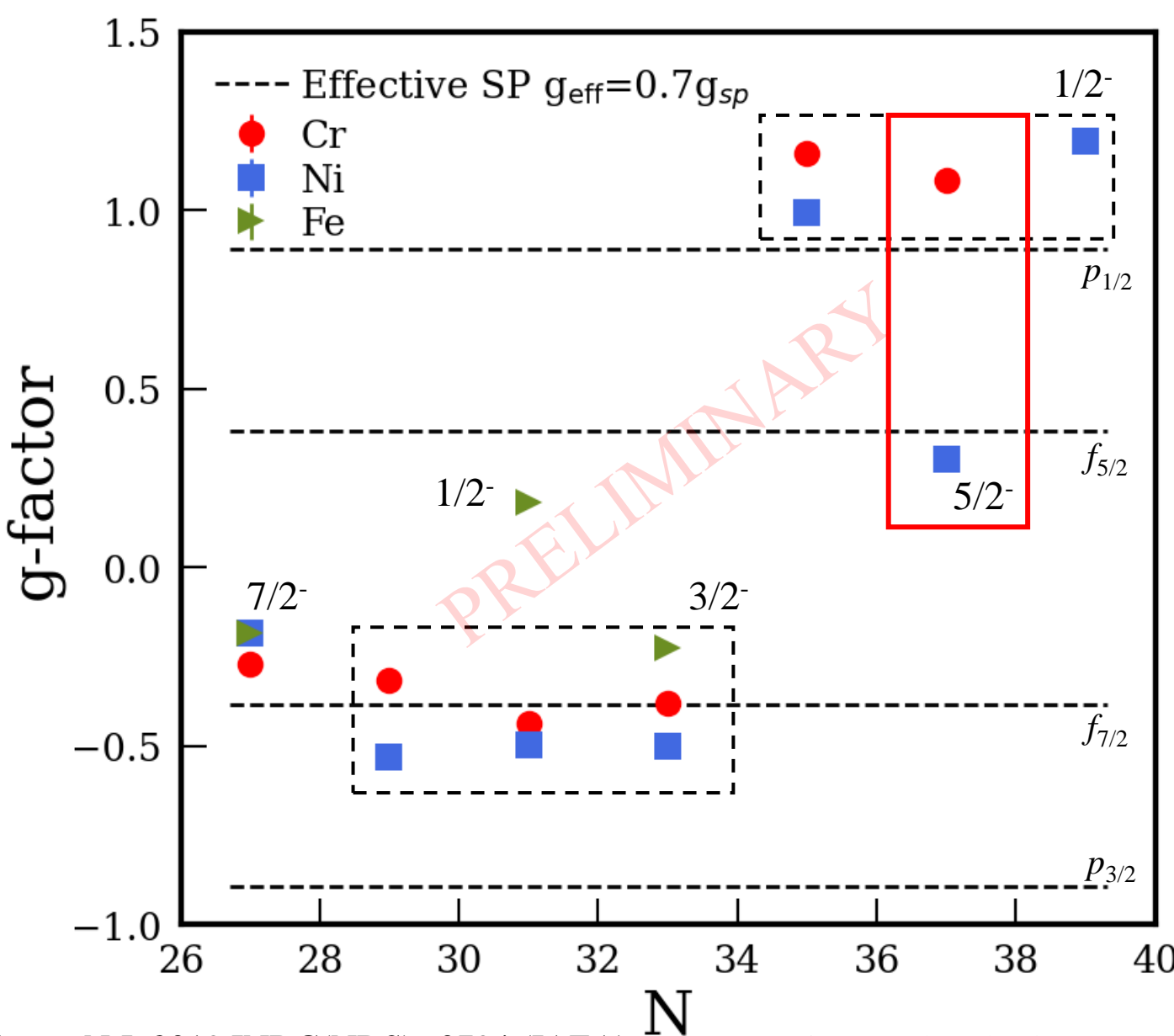
→ Very sensitive to which orbitals are occupied by the valence particles



- $^{51}\text{Cr} (N=27) \rightarrow \nu f_{7/2}$  configuration
- $^{53,55,57}\text{Cr} (N=29, 31, 33) \rightarrow \nu p_{3/2}$  configuration
- $^{59,61}\text{Cr} (N=35, 37) \rightarrow \nu p_{1/2}$  configuration

# Results: g factors of odd-*A* Cr isotopes

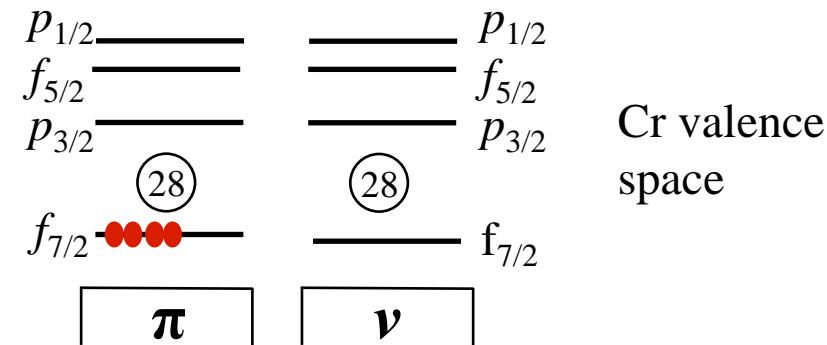
31



g-factor :

$$g = \frac{\mu}{I\mu_N}$$

→ Very sensitive to which orbitals are occupied by the valence particles



- $^{51}\text{Cr} (N=27) \rightarrow \nu f_{7/2}$  configuration
- $^{53,55,57}\text{Cr} (N=29, 31, 33) \rightarrow \nu p_{3/2}$  configuration
- $^{59,61}\text{Cr} (N=35, 37) \rightarrow \nu p_{1/2}$  configuration

$N=37$  config. moving from  $\nu f_{5/2}$  in Ni ( $Z=28$ ) to  $\nu p_{1/2}$  in Cr ( $Z=24$ )

→ Monopole drift of the  $\nu f_{5/2}$  orbital?

# Cr Results: Charge radii of Cr isotopes

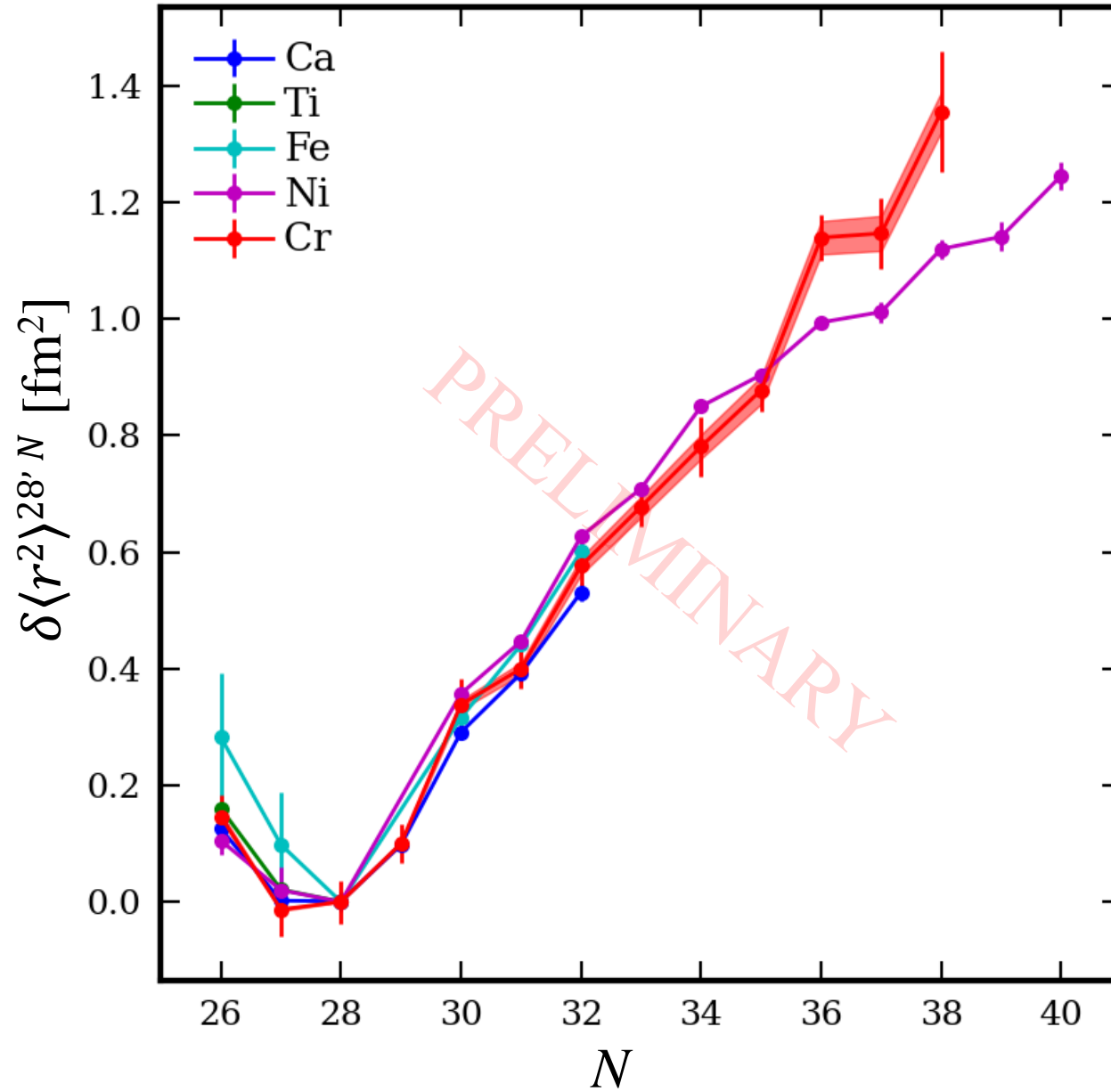
32

$$\delta\nu_i^{A,A'} = \frac{A - A'}{AA'} M_i + F_i \delta\langle r^2 \rangle^{AA'}$$

- F and M determined from King plot using model independent absolute radii values <sup>(1)</sup> (muonic+e<sup>-</sup> scat.)

# Cr Results: Charge radii of Cr isotopes

33

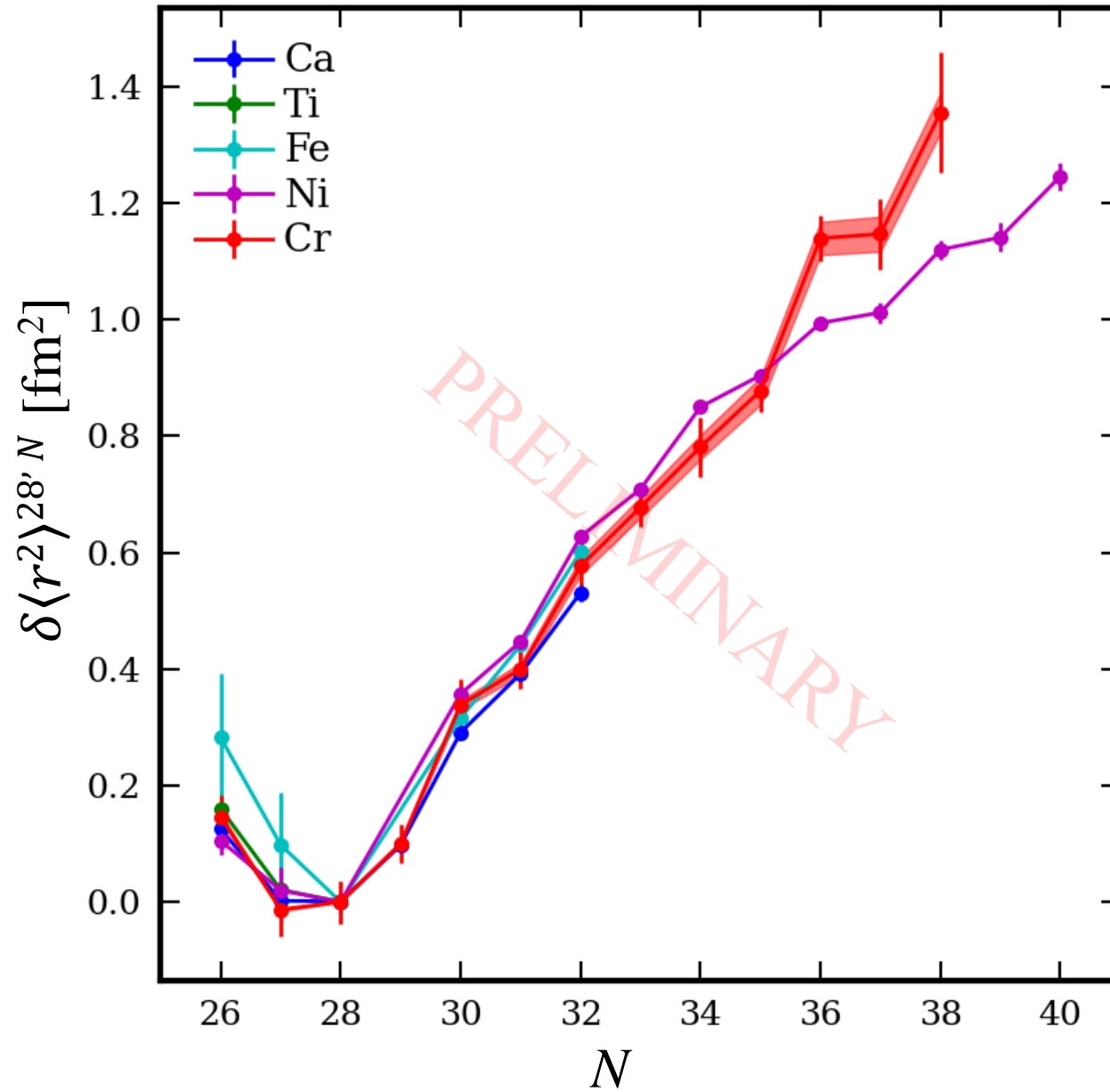


$$\delta \nu_i^{A,A'} = \frac{A - A'}{AA'} M_i + F_i \delta \langle r^2 \rangle^{AA'}$$

- F and M determined from King plot using model independent absolute radii values <sup>(1)</sup> (muonic+e<sup>-</sup> scat.)
- Strong kink observed at N=28, in good agreement with literature
- Steep increase of the Cr charge radii between N=28 and N=32 following closely the Ca trend  
→ Z independent behaviour

# Cr Results: Charge radii of Cr isotopes

34



$$\delta \nu_i^{A,A'} = \frac{A - A'}{AA'} M_i + F_i \delta \langle r^2 \rangle^{AA'}$$

- $F$  and  $M$  determined from King plot using model independent absolute radii values <sup>(1)</sup> (muonic+e<sup>-</sup> scat.)
- Strong kink observed at  $N=28$ , in good agreement with literature
- Steep increase of the Cr charge radii between  $N=28$  and  $N=32$  following closely the Ca trend  
→  $Z$  independent behaviour
- Clear change of slope at  $N=34$  between deformed Cr, and spherical Ni
- Strong odd-even staggering of the Cr radii for  $N>34$

Signature of the beginning of the  $N=40$  Island of Inversion

# The 2023 experimental campaign

35

# “Rotational and hyperfine structure of RaF molecules”

Spokesperson: M. Athanasakis-Kaklamanakis (KU Leuven)  
CERN), S. Wilkins, R. Garzia-Riuz (MIT)  
PhD: Carlos Fajardo-Zambrano (KU Leuven)

# “Collinear resonance ionization spectroscopy of Chromium isotopes between N=28 and N=40”

Spokesperson : L. Lalanne, A. Koszorus (CERN, KU Leuven)

“Probing mag and shell evolution in the vicinity  
of with high-resolution spectroscopy of  $^{81,82}\text{Zn}$ ”  
Spokesperson: X. Yan (Peking Uni.), T. E. Cocolios  
(KU Leuven)  
PhD: Y. Liu (Peking Uni.), D. den Borne (KU  
Leuven)

“Measurement of the changes in the mean-square charge radii of aluminium isotopes across N = 20”  
Spokesperson: A. Koszorus (KU Leuven)  
PhD: J. Reilly (Manchester Uni.)

# RaF for $P,T$ violation searches

36

- electron electric dipole moment (eEDM) : asymmetric charge distribution along electron's spin axis
- Nonzero EDM's implies the existence of the T,P-violating interactions

# RaF for $P,T$ violation searches

37

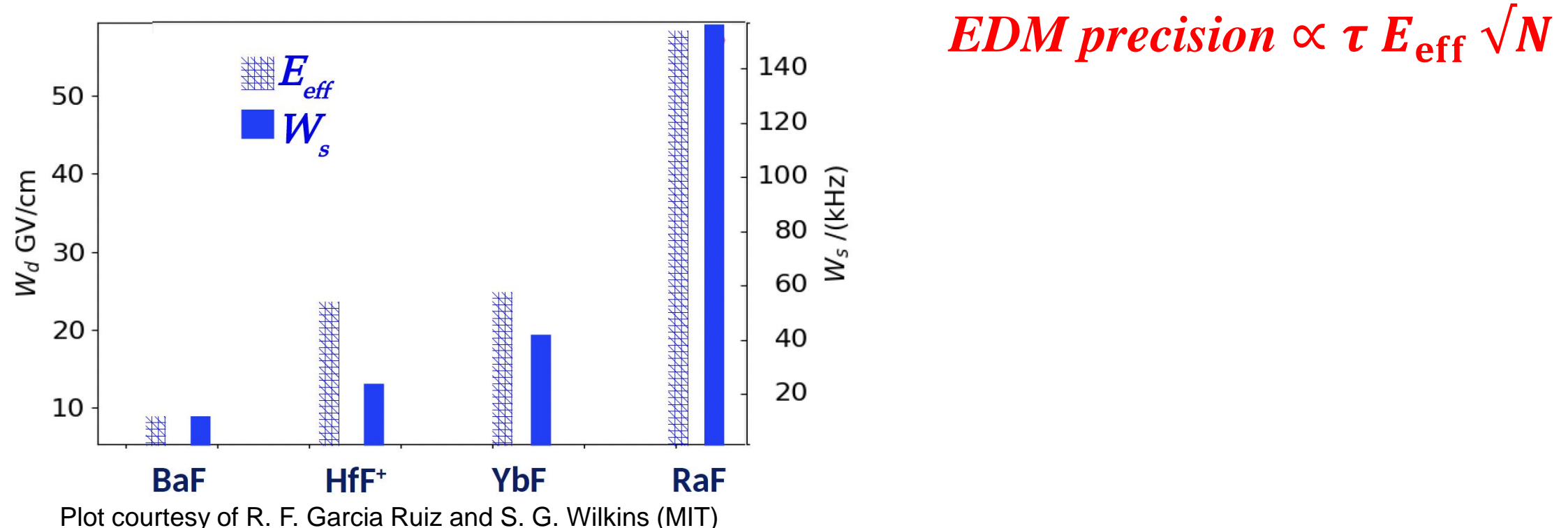
- electron electric dipole moment (eEDM) : asymmetric charge distribution along electron's spin axis
- Nonzero EDM's implies the existence of the T,P-violating interactions

$$\textcolor{red}{EDM \ precision} \propto \tau E_{\text{eff}} \sqrt{N}$$

# RaF for $P,T$ violation searches

38

- electron electric dipole moment (eEDM) : asymmetric charge distribution along electron's spin axis
- Nonzero EDM's implies the existence of the T,P-violating interactions

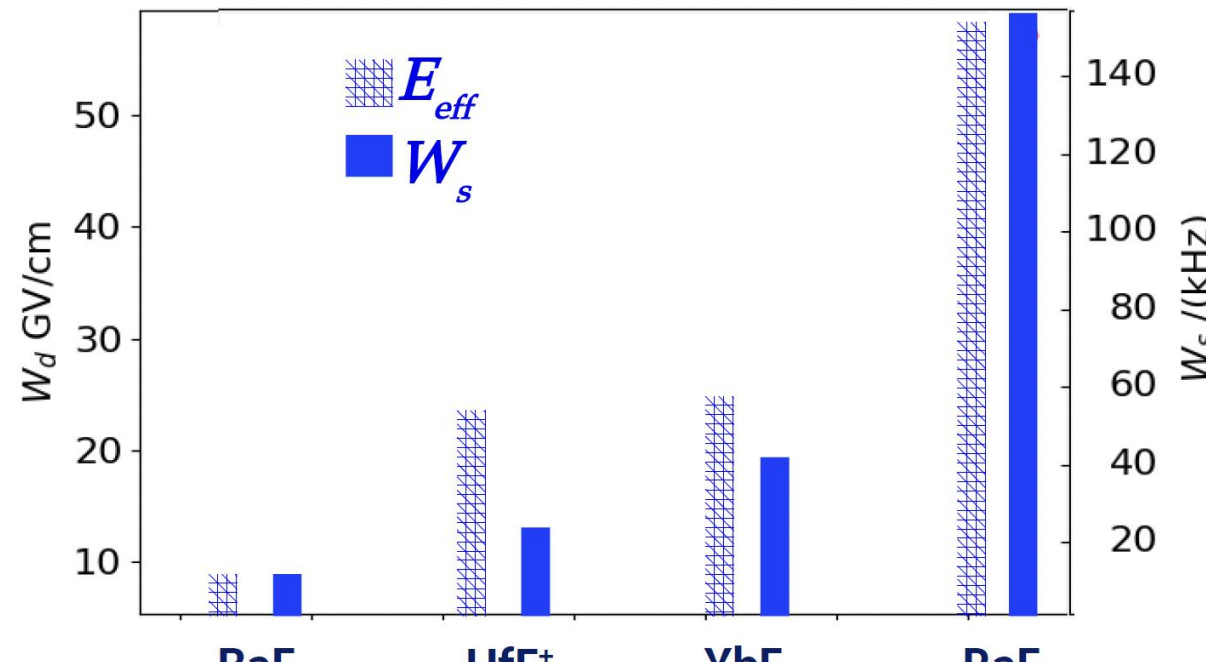


Radioactive molecules:  
Exceptionally sensitive to P,T-violating moments  
 $>10^5$  times more sensitive than stable atoms

# RaF for $P,T$ violation searches

39

- electron electric dipole moment (eEDM) : asymmetric charge distribution along electron's spin axis
- Nonzero EDM's implies the existence of the T,P-violating interactions



Plot courtesy of R. F. Garcia Ruiz and S. G. Wilkins (MIT)

$$\text{EDM precision} \propto \tau E_{\text{eff}} \sqrt{N}$$

Laser coolable in neutral trap!

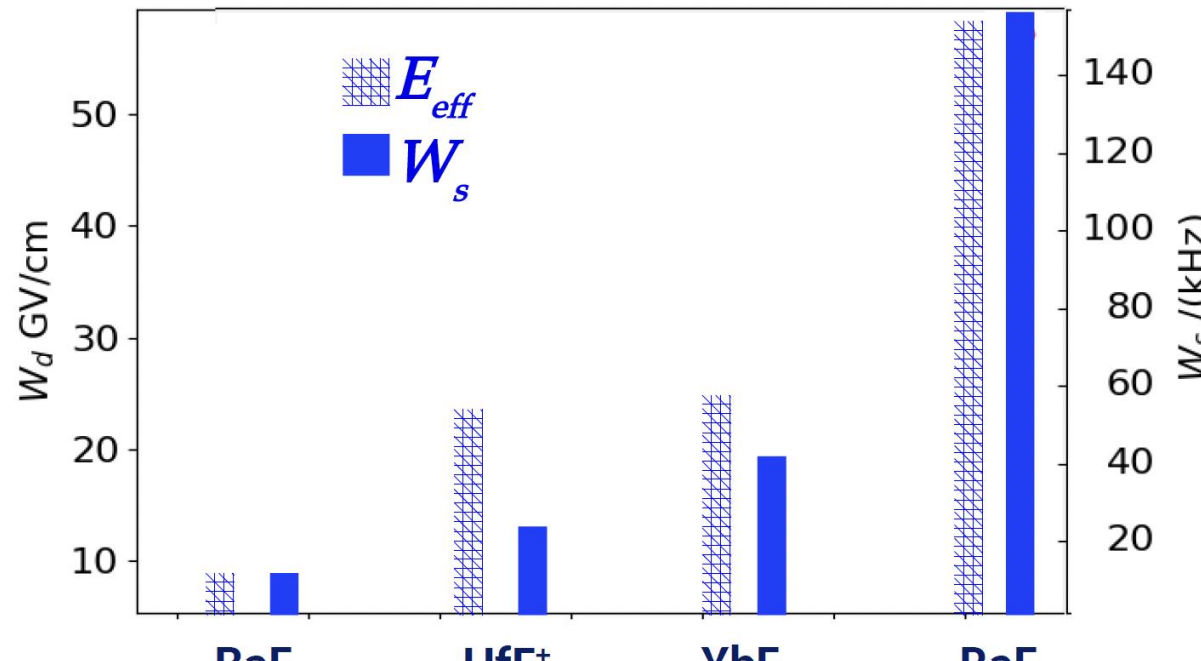


Very long coherence time  $\tau$   
and number density  $N$

Radioactive molecules:  
Exceptionally sensitive to P,T-violating moments  
 $>10^5$  times more sensitive than stable atoms

# RaF for $P,T$ violation searches

- electron electric dipole moment (eEDM) : asymmetric charge distribution along electron's spin axis
- Nonzero EDM's implies the existence of the T,P-violating interactions



Plot courtesy of R. F. Garcia Ruiz and S. G. Wilkins (MIT)

Radioactive molecules:  
Exceptionally sensitive to P,T-violating moments  
 $>10^5$  times more sensitive than stable atoms

$$\text{EDM precision} \propto \tau E_{\text{eff}} \sqrt{N}$$

Laser coolable in neutral trap!



Very long coherence time  $\tau$   
and number density  $N$

→ RaF is one of the most promising system for  $P,T$  violation searches

# High-resolution spectroscopy of RaF

41

The Hamiltonian of RaF:

$$\hat{H}^{\text{RaF}} = \hat{H}_{\text{el}} + \hat{H}_{\text{vib}} + \hat{H}_{\text{rot}} + \hat{H}_{\text{hfs}} + \cdots + \hat{H}_{P,T}$$

# High-resolution spectroscopy of RaF

42

The Hamiltonian of RaF:

$$\hat{H}^{\text{RaF}} = \hat{H}_{\text{el}} + \hat{H}_{\text{vib}} + \hat{H}_{\text{rot}} + \hat{H}_{\text{hfs}} + \cdots + \hat{H}_{P,T}$$



Electronic and vibrational structure

CRIS 2018

Nature 581, 396 (2020)

# High-resolution spectroscopy of RaF

43

The Hamiltonian of RaF:

$$\hat{H}^{\text{RaF}} = \hat{H}_{\text{el}} + \hat{H}_{\text{vib}} + \hat{H}_{\text{rot}} + \hat{H}_{\text{hfs}} + \dots + \hat{H}_{P,T}$$

Electronic and vibrational structure

CRIS 2018

Nature 581, 396 (2020)

Rotational structure

CRIS 2021

Nature Physics, accepted (2023)

PRL 127, 033001 (2021)

[arXiv:2308.14862](https://arxiv.org/abs/2308.14862), submitted (2023)

Magnetic dipole interaction

CRIS 2021

[arXiv:2311.04121](https://arxiv.org/abs/2311.04121), submitted (2023)

See poster of Carlos Fajardo-Zambrano!

# High-resolution spectroscopy of RaF

The Hamiltonian of RaF:

$$\hat{H}^{\text{RaF}} = \hat{H}_{\text{el}} + \hat{H}_{\text{vib}} + \hat{H}_{\text{rot}} + \hat{H}_{\text{hfs}} + \dots + \hat{H}_{P,T}$$

Electronic and vibrational structure

CRIS 2018

Nature 581, 396 (2020)

Rotational structure

CRIS 2021

Nature Physics, accepted (2023)

PRL 127, 033001 (2021)

[arXiv:2308.14862](https://arxiv.org/abs/2308.14862), submitted (2023)

Magnetic dipole interaction

CRIS 2021

arXiv:2311.04121, submitted (2023)

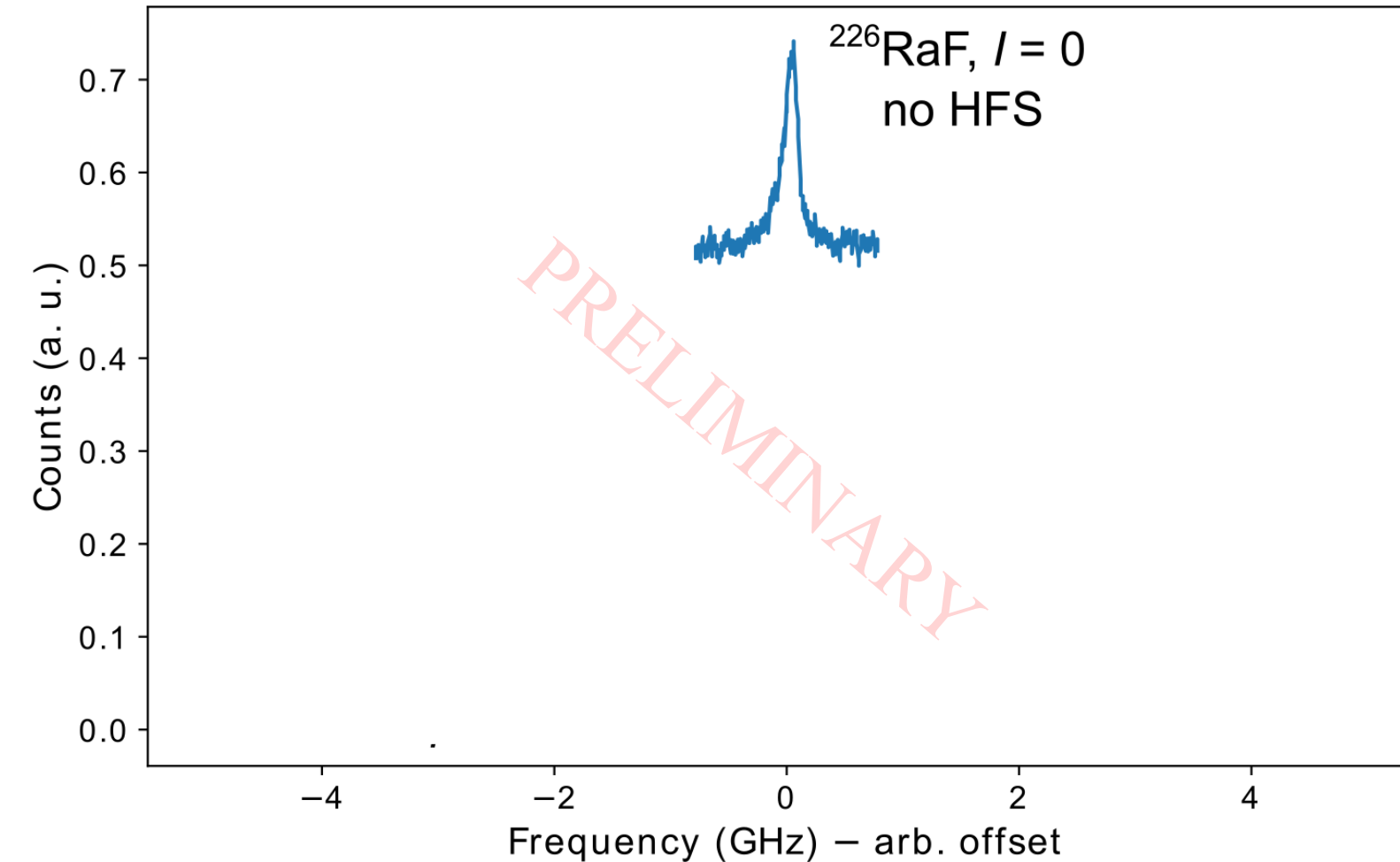
See poster of Carlos Fajardo-Zambrano!

Electric quadrupole interaction

CRIS 2023

# High-resolution spectroscopy of RaF

45

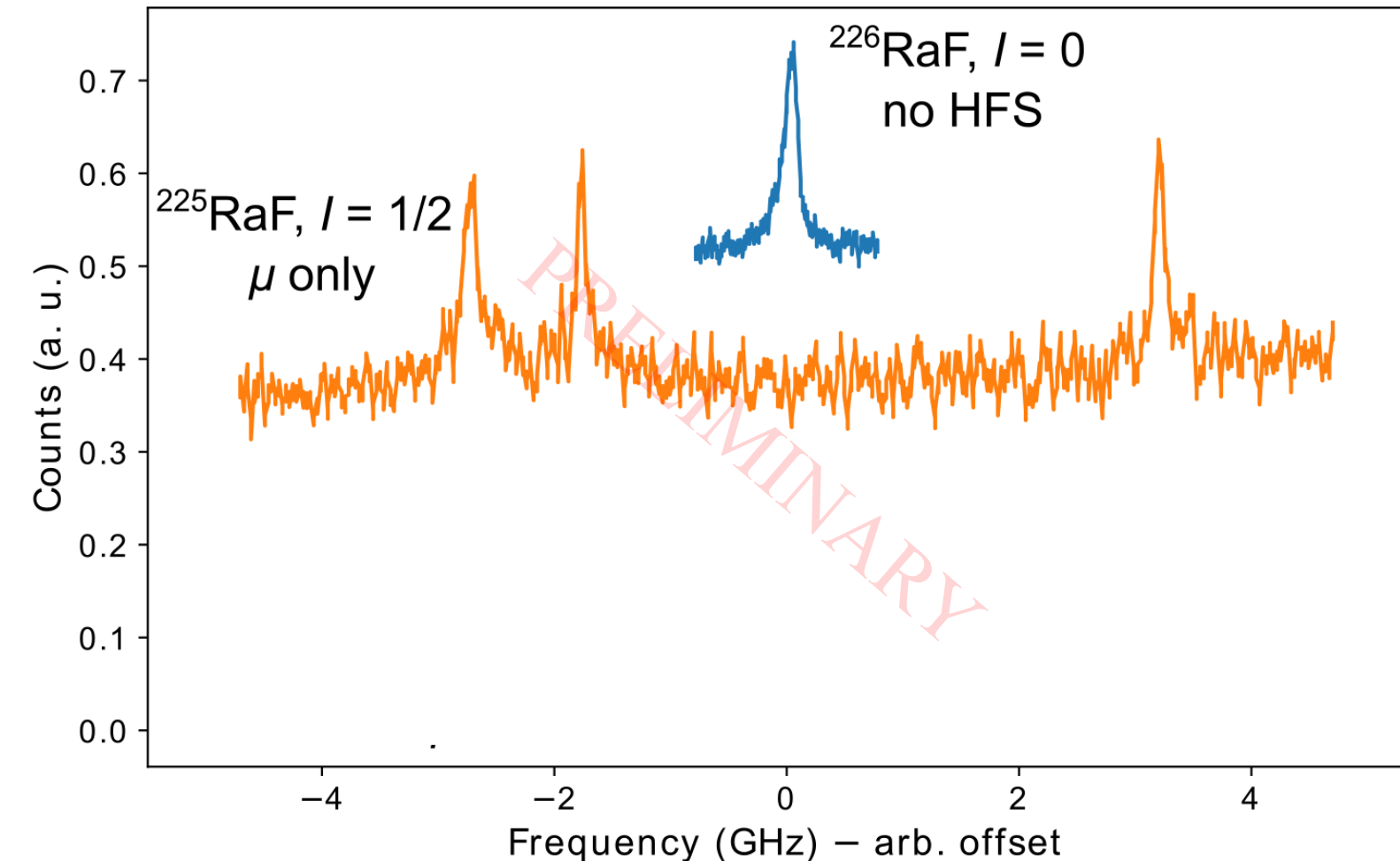


2023 RaF:

- High res. spec. of  $^{226}\text{RaF}$

# High-resolution spectroscopy of RaF

46

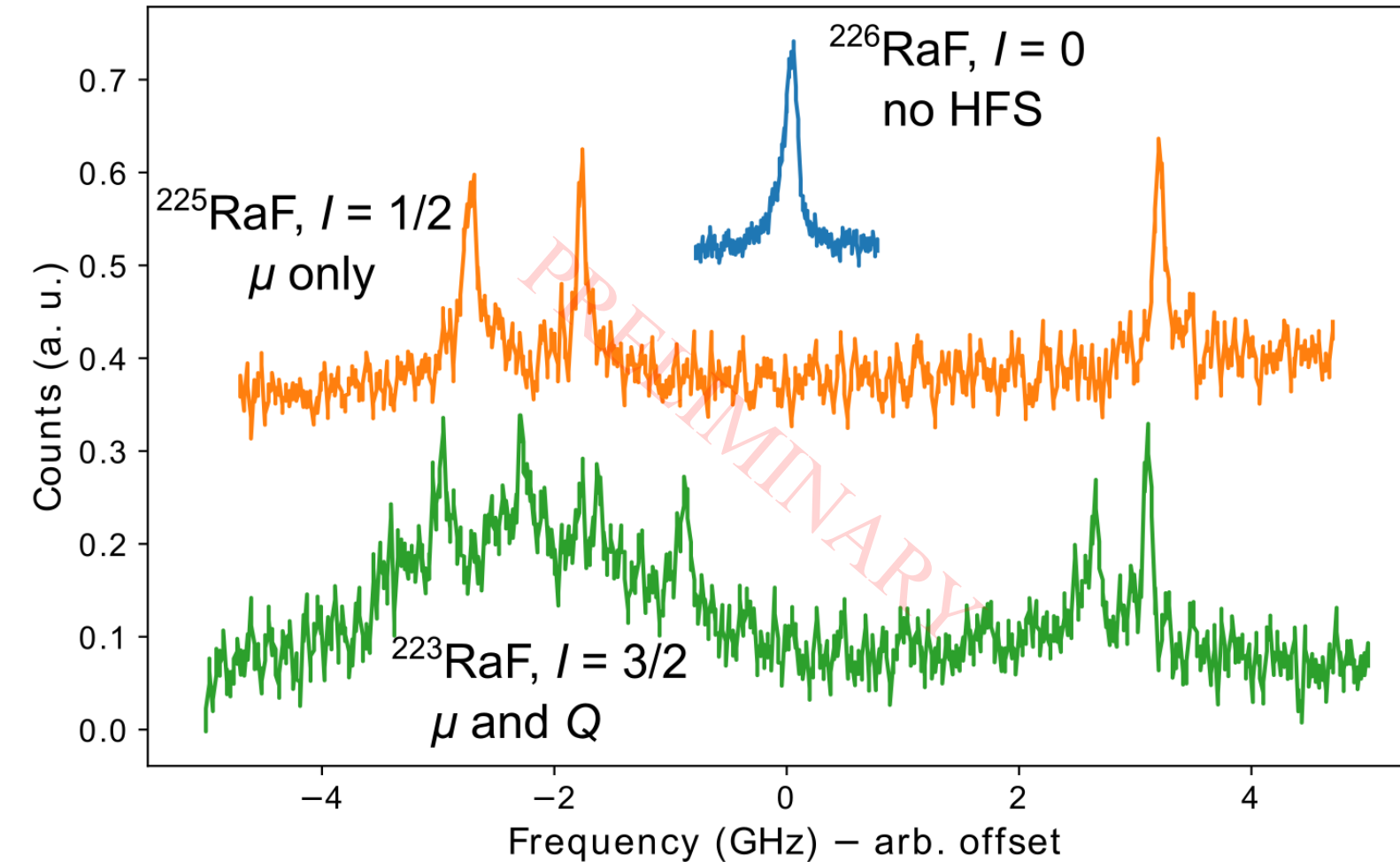


2023 RaF:

- High res. spec. of  $^{226,225}\text{RaF}$

# High-resolution spectroscopy of RaF

47



2023 RaF:

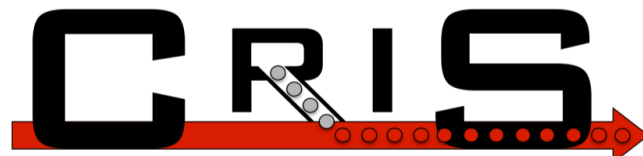
- High res. spec. of  $^{226,225,223}\text{RaF}$
- First measurement of the hyperfine structure of  $^{223}\text{RaF}$

→ Analysis ongoing for the first measurement of an electric quadrupole moment in a radioactive molecule

# Conclusion

48

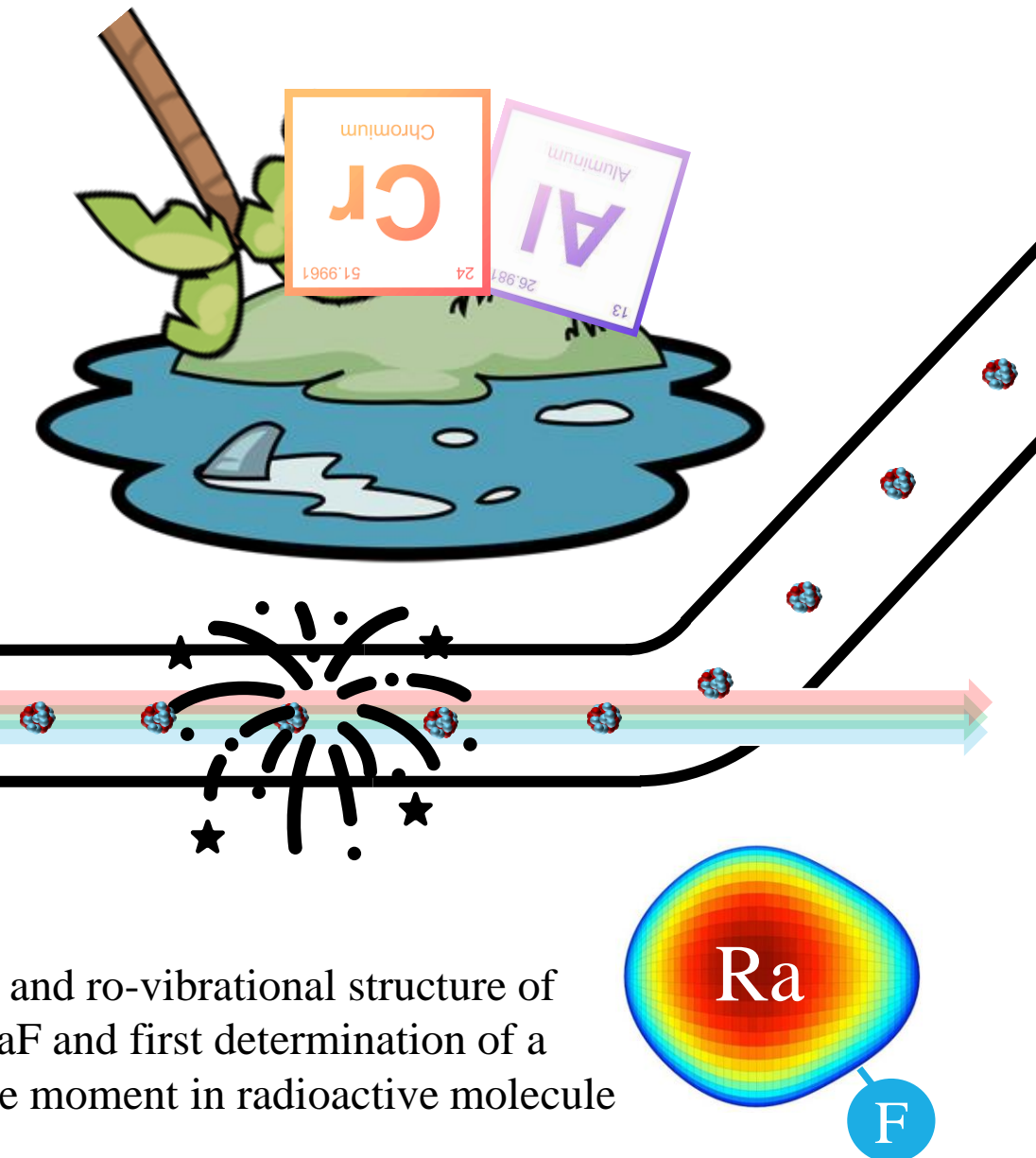
2023 @



- Two major upgrades: New end of the beam line and new Decay spectroscopy station successfully commisioned
- Charge radii of neutron rich Aluminium isotopes across  $N=20$  in the Island of inversion
- Spin, radii and magnetic dipole moment of neutron rich Chromium isotopes from  $N=26$  to  $N=38$ , entering the  $N=40$  Island of Inversion
- Spin, Radii and moments of  $^{81,82}\text{Zn}$  across  $N=50$  in the vicinity of  $^{78}\text{Ni}$

See talk of Yongchao Liu !

- Hyperfine and ro-vibrational structure of  $^{223,225,226}\text{RaF}$  and first determination of a quadrupole moment in radioactive molecule



# The 2023 CRIS Collaboration

49



O. Ahmad, M. Au, **M. Athanasakis-Kaklamanakis**, J. Berbalk, C. Bernerd, K. Chrysalidis,  
T. E. Cocolios, R. van Duyse, R. P. de Groote, C. Fajardo-Zambrano, K. T. Flanagan, S. Franchoo,  
R. F. Garcia Ruiz, R. Heinke, M. Heines, D. Hanstorp, P. Imgram, Á. Koszorús, **L. Lalanne**,  
P. Lassegues, R. Lica, J. Lim, **Y. Liu**, K. Lynch, R. Mancheva, **A. McGlone**, W. Mei, G. Neyens,  
L. Nies, A. Raggio, **J. Reilly**, S. Rothe, E. Smets, **B. van den Borne**, J. Warbinek, J. Wessolek,  
S. Wilkins, X. F. Yang



Massachusetts  
Institute of  
Technology



北京大学  
PEKING UNIVERSITY



UNIVERSITY OF  
GOTHENBURG



THANK YOU FOR  
YOUR  
ATTENTION